JACS
JOURNAL OF THE AMERICAN CHEMICAL SOCIETY

Article

pubs.acs.org/JACS

Enterobactin-Mediated Delivery of β-Lactam Antibiotics Enhances Antibacterial Activity against Pathogenic *Escherichia coli*

Tengfei Zheng and Elizabeth M. Nolan*

Department of Chemistry, Massachusetts Institute of Technology, Cambridge, Massachusetts 02139, United States

Supporting Information

ABSTRACT: The design, synthesis, and characterization of enterobactin−antibiotic conjugates, hereafter Ent-Amp/Amx, where the β-lactam antibiotics ampicillin (Amp) and amoxicillin (Amx) are linked to a monofunctionalized enterobactin scaffold via a stable poly(ethylene glycol) linker are reported. Under conditions of iron limitation, these siderophore-modified antibiotics provide enhanced antibacterial activity against *Escherichia coli* strains, including uropathogenic *E. coli* CFT073 and UTI89, enterohemorrhagic *E. coli* O157:H7, and enterotoxigenic *E. coli* O78:H11, compared to the parent β-lactams. Studies with *E. coli* K-12 derivatives defective in ferric enterobactin transport reveal that the enhanced antibacterial activity observed for this strain requires the outer membrane ferric enterobactin transporter FepA. A remarkable 1000-fold decrease in minimum inhibitory concentration (MIC) value is observed for uropathogenic *E. coli* CFT073 relative to Amp/Amx, and time-kill kinetic studies demonstrate that Ent-Amp/Amx kill this strain more rapidly at 10-fold lower concentrations than the parent antibiotics. Moreover, Ent-Amp and Ent-Amx selectively kill *E. coli* CFT073 co-cultured with other bacterial species such as *Staphylococcus aureus*, and Ent-Amp exhibits low cytotoxicity against human T84 intestinal cells in both the apo and iron-bound forms. These studies demonstrate that the native enterobactin platform provides a means to effectively deliver antibacterial cargo across the outer membrane permeability barrier of Gram-negative pathogens utilizing enterobactin for iron acquisition.

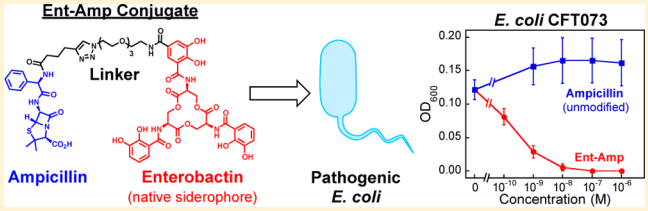

INTRODUCTION

Bacterial infections as well as the emergence and spread of antibiotic resistance in human pathogens are serious public health problems in hospital and community settings across the globe.[1] New strategies to prevent and treat bacterial infections are needed, including methods to overcome antibacterial resistance that results from the outer membrane permeability barrier in Gram-negative organisms and targeting approaches that afford species- or pathogen-specific therapeutics.[2−8]

Metal ions are essential nutrients for all organisms. Almost all bacterial species have a metabolic iron requirement and therefore employ various strategies to acquire this metal ion when colonizing.[9,10] Siderophores are high-affinity Fe(III) chelators that are produced by bacteria under conditions of iron limitation, such as those encountered in the vertebrate host, to scavenge this metal ion from the environment.[10,11] Siderophore producers also express dedicated ferric siderophore import machinery and employ various mechanisms to release siderophore-bound iron following cellular uptake (e.g., reductive and/or hydrolytic release mediated by reductases and/or esterases, respectively).[12] Numerous studies support the importance of siderophore-based iron acquisition during bacterial infections.[13−19] Thus, the potential of using siderophores,[20−25] or targeting siderophore biosynthetic and transport machineries,[26−28] in therapeutic development continues to attract significant interest. Of particular relevance to the advances described herein are prior investigations pertaining to the development of siderophore−antibiotic conjugates for "Trojan horse" antibiotic delivery.[29−58] This strategy has received particular attention for the delivery of antibiotics into Gram-negative bacteria because these organisms are inherently less sensitive to many antibiotics used in the clinic as a result of the outer membrane permeability barrier.[6−8]

Both native siderophores and synthetic siderophore mimics have been evaluated as platforms for therapeutic development.[20−25,59,60] In the clinic, the native siderophore desferrioxamine B is used for iron-chelation therapy in patients with iron overload. Several antibiotic small molecules found in Nature called "sideromycins" provide inspiration for synthetic siderophore−antibiotic conjugates.[61] The sideromycins are secondary metabolites comprised of a siderophore moiety and a toxic cargo; the siderophore portion targets sideromycins to bacterial strains expressing the appropriate siderophore receptor. Microcin E492m, a siderophore−antibiotic conjugate produced by a clinical isolate of *Klebsiella pneumoniae*, is an 84-residue antibacterial peptide with a glucosylated enterobactin (Ent, Figure 1) derivative attached to its C-terminus that exhibits enhanced antibacterial activity against strains expressing the enterobactin receptor FepA.[62] From the standpoints of antibacterial activity and therapeutic potential, studies of synthetic siderophore−antibiotic conjugates have provided

Received: April 18, 2014
Published: June 13, 2014

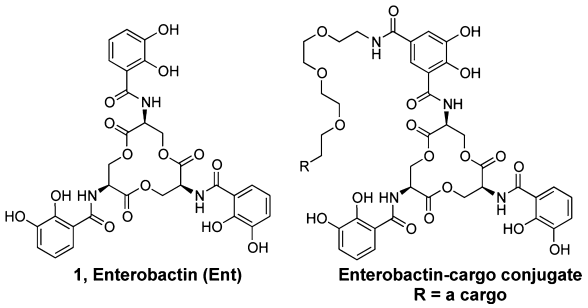

Figure 1. Structures of enterobactin (**1**, Ent) and a generalized enterobactin–cargo conjugate.

the community with mixed results, causing some skepticism about the potential of siderophore-based approaches despite the successful utilization of such molecules by Nature.

Many of the failures encountered with early and recent studies of siderophore-based antibiotic delivery may be attributed, at least in part, to (i) use of non-native siderophores with relatively low Fe(III) affinities and/or compromised receptor recognition;[63] (ii) modification of antibiotics such that the antibacterial activity is attenuated or lost completely;[42,44,51,58] (iii) bridging the siderophores and antibiotics with problematic linkers, including linkers designed for drug release that are either too stable or too labile, the latter of which promotes premature release;[25,45−48] and (iv) antibiotic resistance.[34,63] Nevertheless, the lessons of many unsuccessful studies highlight the complexity of siderophore-based therapeutic development and provide a foundation for inventing improved next-generation approaches. Many of the issues described above may be overcome by careful molecular design and biological evaluation. In particular, the selection of appropriate native siderophore platforms and modification of these platforms in ways that do not compromise iron binding or receptor recognition, installation of an antibacterial cargo in such a manner that antibacterial activity is retained, and the development and application of assays that afford insight into the fate of siderophore–antibiotic conjugates are critical to the overall success of this approach. Along such lines, a recent and insightful study by Pfizer addressed complications associated with using relatively low-molecular-weight siderophore mimics *in vivo*.[63] Their results indicate that competition between the siderophore-conjugated monobactam MB-1 and native siderophores resulted in poor *in vivo* efficacy against *Pseudomonas aeruginosa* and provide support for designing and evaluating siderophore–antibiotic conjugates based on native siderophore platforms. One recent and successful example based on a native siderophore platform is a mycobactin–artemisinin conjugate that exhibits enhanced antibacterial activity against *Mycobacterium tuberculosis* compared to unmodified artemisinin.[64]

Enterobactin (Ent, Figure 1) is a triscatecholate siderophore biosynthesized by enteric bacteria and used for iron acquisition in the vertebrate host.[65] Motivated by the importance of Ent in the host/microbe interaction as well as the decades of investigations pertaining to its (bio)synthesis, coordination chemistry, and biology, in prior work we reported a synthetic route to monofunctionalized Ent platforms.[66] Moreover, we established that the native Ent platform, when monofunctionalized at the C5 position of one catecholate ring (Figure 1), affords delivery of nontoxic small-molecule cargo across the outer membrane of Gram-negative organisms that express Ent uptake machinery (e.g., FepABCDG of *Escherichia coli*).[66] As described herein, this proof-of-concept study motivated us to demonstrate that Ent effectively delivers antibacterial cargo to organisms that utilize Ent for iron acquisition, thereby providing antibiotic targeting to specific sub-populations and a means to address antibiotic resistance that results from the Gram-negative outer membrane permeability barrier.

In this work, we present the syntheses and characterization of siderophore–antibiotic conjugates based on the native Ent platform that harbor the clinically relevant β-lactam antibiotics ampicillin (Amp) and amoxicillin (Amx). These antibiotics block cell wall biosynthesis by inhibiting transpeptidases, also named penicillin binding proteins (PBPs), located in the periplasm of *E. coli*. We report that the Ent-β-lactam conjugates exhibit significantly enhanced antibacterial activity (up to 1000-fold) against pathogenic *E. coli* and provide more rapid cell-killing than the parent β-lactams as a result of Ent-mediated delivery to the periplasm. Moreover, in proof-of-concept studies for species-specific killing, these conjugates selectively kill *E. coli* in the presence of *Staphylococcus aureus*, a Gram-positive organism that is more susceptible to the parent β-lactams. These studies support the notion that native siderophore platforms provide an effective means to target molecular cargo to siderophore-utilizing organisms and to hijack siderophore uptake machinery to deliver cargos, including antibiotics, across the outer membrane permeability barrier of Gram-negative microbes.

EXPERIMENTAL SECTION

Synthetic Reagents. Dimethylformamide (DMF) and dichloromethane (CH_2Cl_2) were obtained from a VAC solvent purification system (Vacuum Atmospheres). Anhydrous dimethyl sulfoxide (DMSO) was purchased from Sigma-Aldrich and used as received. HPLC-grade acetonitrile (MeCN) was purchased from EMD. L-Ent **1**,[67] the D-enantiomer of benzyl-protected Ent-CO_2H **2**, and the benzyl-protected Ent-PEG_3-N_3 **3** were synthesized according to previously reported procedures.[66] 11-Azido-3,6,9-trioxaundecan-1-amine was purchased from Fluka. All other chemicals and solvents were purchased from Sigma-Aldrich or Alfa Aesar in the highest available purity and used as received. General synthetic methods are provided as Supporting Information.

***N1*-(2-(2-(2-(2-Azidoethoxy)ethoxy)ethoxy)ethyl)-*N3*-((3*S*,7*S*,11*S*)-7,11-bis(2,3-dihydroxybenzamido)-2,6,10-trioxo-1,5,9-trioxacyclododecan-3-yl)-4,5-dihydroxyisophthalamide (4).** Benzyl-protected Ent-azide **3** (80 mg, 55 μmol) and pentamethylbenzene (PMB, 147 mg, 990 μmol) were dissolved in 5 mL of anhydrous CH_2Cl_2 to give a light yellow solution. This solution was cooled to −78 °C in an acetone/dry ice bath under N_2, and BCl_3 (660 μL of 1 M solution in CH_2Cl_2, 660 μmol) was added slowly along the flask wall. After the solution was stirred for 1.5 h, DIPEA (300 μL, 1.73 mmol) was added to the flask, followed by MeOH (2 mL) to quench the reaction. The reaction was then warmed to room temperature, and the solvents were removed under reduced pressure. The resulting white solid was dissolved in 5:3 MeOH/1,4-dioxane and purified by preparative HPLC (33% B for 5 min and 33−60% B over 20 min, 10 mL/min). The product eluted at 17 min and was lyophilized to yield compound **4** as white solid (13.9 mg, 28%). ^{1}H NMR (DMSO-d_6, 500 MHz): δ 3.35−3.57 (16H, m), 4.38−4.41 (3H, m), 4.63−4.69 (3H, m), 4.89−4.96 (3H, m), 6.74 (2H, dd, J = 7.5, 8.0 Hz), 6.97 (2H, d, J = 7.5 Hz), 7.35 (2H, d, J = 8.0 Hz), 7.46 (1H, s), 7.94 (1H, s), 8.33−8.35 (1H, m), 9.12 (2H, d, J = 6.0 Hz), 9.29 (1H, d, J = 6.0 Hz), 9.44 (2H, bs), 9.76 (1H, bs), 11.6 (2H, bs), 11.9 (1H, bs). ^{13}C NMR ($CDCl_3$, 125 MHz): δ 50.1, 51.5, 63.6, 69.1, 69.4, 69.8, 69.8, 69.9, 69.9, 115.3, 115.4, 115.4, 117.7, 118.5, 118.7, 119.4, 125.2, 145.9, 146.3, 148.7, 148.7, 150.8, 166.0, 168.4, 169.1, 169.6, 169.7. IR (KBr disk, cm^{-1}): 3389, 2954, 2928, 2868, 2111, 1754, 1645, 1589, 1535, 1460, 1384, 1329, 1266, 1176, 1132, 1074, 992, 846. HRMS (ESI): $[M+Na]^+$ m/z calcd 932.2506, found 932.2520.

dx.doi.org/10.1021/ja503911p | J. Am. Chem. Soc. 2014, 136, 9677−9691

***N1*-(2-(2-(2-(2-Azidoethoxy)ethoxy)ethoxy)ethyl)-4,5-bis-(benzyloxy)-*N3*-((3*R*,7*R*,11*R*)-7,11-bis(2,3-bis(benzyloxy)-benzamido)-2,6,10-trioxo-1,5,9-trioxacyclododecan-3-yl)-isophthalamide (5).** 11-Azido-3,6,9-trioxaundecan-1-amine (36 μL, 181 μmol) and D-Bn_6Ent-COOH (**2**, 177 mg, 142 μmol) were dissolved in 5 mL of dry CH_2Cl_2. PyAOP (147 mg, 283 μmol) and DIPEA (98.5 μL, 568 μmol) were added to give a light yellow solution. The reaction was stirred for 4 h at room temperature and concentrated, and the crude product was purified by preparative TLC (50% EtOAc/CH_2Cl_2) to afford **5** as white foam (159 mg, 77%). TLC R_f = 0.6 (10% MeOH/CH_2Cl_2). ^{1}H NMR (DMSO-d_6, 500 MHz): δ 3.33 (2H, *J* = 5.2 Hz), 3.62−3.69 (14H, m), 4.02−4.06 (3H, m), 4.15−4.18 (3H, m), 4.91−4.94 (3H, m), 5.04−5.21 (12H, m), 6.96 (1H, s), 7.11−7.45 (36H, m), 7.65−7.67 (2H, m), 7.85−7.85 (1H, m), 7.97−7.97 (1H, m), 8.50−8.54 (3H, m). ^{13}C NMR ($CDCl_3$, 125 MHz): δ 25.6, 29.5, 38.8, 40.0, 45.3, 51.3, 51.4, 63.9, 64.1, 69.8, 39.8, 70.0, 70.3, 70.4, 70.4, 71.2, 71.2, 76.3, 76.3, 116.8, 117.5, 120.4, 123.0, 124.3, 125.4, 126.1, 126.2, 127.6, 127.6, 127.9, 128.2, 128.3, 128.4, 128.4, 128.5, 128.5, 128.6, 128.6, 128.8, 128.8, 128.9, 129.0, 130.1, 135.4, 135.7, 135.9, 136.0, 136.1, 146.8, 146.9, 149.1, 151.6, 151.8, 164.3, 164.9, 164.9, 165.8, 168.9, 169.0, 169.1, 176.2. IR (KBr disk, cm^{-1}): 3357, 3062, 3032, 2958, 2923, 2859, 2104, 1751, 1551, 1576, 1515, 1455, 1375, 1345, 1299, 1264, 1204, 1126, 1082, 1040, 1018, 957, 915, 854, 811. HRMS (ESI): $[M+H]^+$ *m*/*z* calcd 1476.5323, found 1476.5318.

***N*1-(2-(2-(2-(2-Azidoethoxy)ethoxy)ethoxy)ethyl)-*N*3-((3*R*,7*R*,11*R*)-7,11-bis(2,3-dihydroxybenzamido)-2,6,10-trioxo-1,5,9-trioxacyclododecan-3-yl)-4,5-dihydroxyisophthalamide (6).** Compound **6** was synthesized from **5** (153 mg, 105 μmol) following the same procedure as for compound **4**. The crude reaction was purified by preparative HPLC (33% B for 5 min and 33−60% B over 20 min, 10 mL/min). The product eluted at 17.0 min and was lyophilized to yield compound **6** as white solid (31 mg, 33%). ^{1}H NMR ($CDCl_3$, 500 MHz): δ 3.34−3.56 (16H, m), 4.39−4.41 (3H, m), 4.61−4.66 (3H, m), 4.88−4.94 (3H, m), 6.74 (2H, dd, *J* = 7.8, 7.8 Hz), 6.96 (2H, d, *J* = 7.8 Hz), 7.33 (2H, d, *J* = 7.8 Hz), 7.44 (1H, s), 7.91 (1H, s), 8.31−8.33 (1H, m), 9.12−9.13 (2H, m), 9.27−9.28 (1H, m), 9.50 (2H, bs), 9.84 (1H, bs), 11.6 (2H, bs), 11.9 (1H, bs). ^{13}C NMR ($CDCl_3$, 125 MHz): δ 50.1, 51.5, 63.6, 69.1, 69.4, 69.8, 69.8, 69.9, 69.9, 115.3, 115.4, 115.4, 117.7, 118.5, 118.7, 119.4, 125.2, 145.9, 146.3, 148.7, 148.7, 150.8, 166.0, 168.4, 169.1, 169.6, 169.7. IR (KBr disk, cm^{-1}): 3390, 2958, 2925, 2863, 2110, 1754, 1645, 1589, 1535, 1460, 1384, 1342, 1262, 1176, 1117, 1074, 841, 800. HRMS (ESI): $[M+Na]^+$ *m*/*z* calcd 936.2506, found 936.2512.

(2*S*,5*R*,6*R*)-6-((*R*)-2-(Hex-5-ynamido)-2-phenylacetamido)-3,3-dimethyl-7-oxo-4-thia-1-azabicyclo[3.2.0]heptane-2-carboxylic Acid (7). 5-Hexynoic acid (113 μL, 1.00 mmol) and thionyl chloride (1.00 mL, 13.8 mmol) were combined and refluxed for 1 h. The reaction was cooled to room temperature and concentrated under reduced pressure, and the resulting crude acyl chloride was dissolved in acetone (0.5 mL) and carried on to the next step without purification. Ampicillin sodium salt (186 mg, 0.500 mmol) was dissolved in a solution of $NaHCO_3$ (210 mg, 2.5 mmol) in 4:1 water/acetone (2.5 mL) and cooled on ice, to which the acyl chloride was added slowly with stirring. The reaction was subsequently warmed to room temperature and stirred for 1 h. Water (3 mL) was added to the reaction, and the aqueous phase was washed with EtOAc (2 × 10 mL), acidified to pH 2 by addition of HCl, and extracted with EtOAc (20 mL). The resulting organic phase was washed with cold water (2 × 5 mL), dried over Na_2SO_4, and concentrated under reduced pressure. The crude reaction was triturated with hexanes, which afforded a yellow solid (180 mg, 77%). This solid was used in the following steps without further purification. TLC R_f = 0.1 (10% MeOH/CH_2Cl_2). ^{1}H NMR (DMSO-d_6, 500 MHz): δ 1.41 (3H, s), 1.55 (3H, s), 1.64−1.69 (2H, m), 2.13−2.16 (2H, m), 2.29−2.32 (2H, m), 2.77−2.78 (1H, m), 4.20 (1H, s), 5.39 (1H, d, *J* = 4.0 Hz), 5.52 (1H, dd, *J* = 4.0, 8.0 Hz), 5.70 (1H, d, *J* = 8.0 Hz), 7.25−7.43 (5H, m), 8.57 (1H, d, *J* = 8.0 Hz), 9.11 (1H, d, *J* = 8.0 Hz). ^{13}C NMR (DMSO-d_6, 125 MHz): δ 17.4, 24.4, 26.6, 30.4, 33.8, 55.5, 58.1, 63.7, 67.3, 70.3, 71.5, 84.2, 127.2, 127.6, 128.2, 138.2, 169.0, 170.2, 171.5, 173.5. IR (KBr disk, cm^{-1}): 3297, 3058, 3023, 2970, 2937, 2863, 2626, 2526, 2120, 1780, 1688, 1518,1455, 1437, 1390, 1373, 1324, 1295, 1208, 1139, 1027, 1001, 843. HRMS (ESI): $[M+H]^+$ *m*/*z* calcd 444.1588, found 444.1585.

(2*S*,5*R*,6*R*)-6-((*R*)-2-(Hex-5-ynamido)-2-(4-hydroxyphenyl)-acetamido)-3,3-dimethyl-7-oxo-4-thia-1-azabicyclo[3.2.0]-heptane-2-carboxylic Acid (8). Compound **8** was synthesized as described for compound **7** except that amoxicillin (760 mg, 2.1 mmol) was used instead of ampicillin sodium salt. Compound **8** was obtained as light yellow solid (533 mg, 56%) after trituration and employed without further purification. TLC R_f = 0.1 (10% MeOH/CH_2Cl_2). ^{1}H NMR (DMSO-d_6, 500 MHz): δ 1.42 (3H, s), 1.56 (3H, s), 1.63−1.68 (2H, m), 2.12−2.15 (2H, m), 2.25−2.29 (2H, m), 2.76−2.78 (1H, m), 4.19 (1H, s), 5.39 (1H, d, *J* = 4.0 Hz), 5.51−5.54 (2H, m), 6.69 (2H, d, *J* = 8.5 Hz), 7.19 (2H, d, *J* = 8.5 Hz), 8.41 (1H, d, *J* = 8.0 Hz), 8.93 (1H, d, *J* = 8.0 Hz), 9.40 (1H, bs). ^{13}C NMR (DMSO-d_6, 125 MHz): δ 17.6, 24.5, 26.8, 30.4, 34.0, 55.4, 58.2, 63.9, 71.6, 71.7, 84.4, 115.1, 128.4, 128.7, 128.8, 157.0, 169.2, 170.9, 171.7, 173.8. IR (KBr disk, cm^{-1}): 3356, 3294, 3045, 2970, 2928, 1770, 1738, 1650, 1615, 1515, 1457, 1373, 1208, 1009, 945, 839, 815. HRMS (ESI): $[M+Na]^+$ *m*/*z* calcd 460.1537, found 460.1534.

(4*S*)-2-(((*R*)-2-(Hex-5-ynamido)-2-phenylacetamido)methyl)-5,5-dimethylthiazolidine-4-carboxylic Acid (9). Compound **7** (60 mg, 0.13 mmol) was dissolved in 1:1 H_2O/MeCN (5 mL), and TFA was added to a final concentration of 1%. The solution was incubated at 37 °C for 24 h and purified by preparative HPLC (20−50% B over 25 min, 10 mL/min), which afforded a white powder (12 mg, 25%). The white powder is a diastereomeric mixture of products, and no further separation was performed. ^{1}H NMR (DMSO-d_6, 500 MHz): δ (mixture of two diastereomers) 1.22−1.23 (3H, pair of s), 1.54−1.58 (3H, pair of s), 1.62−1.68 (2H, m), 2.12−2.14 (2H, m), 2.28−2.30 (2H, m), 2.77 (1H, s), 3.18−3.24 (0.5H, m), 3.30−3.36 (0.5H, m), 3.44−3.49 (0.5H, m), 3.55−3.60 (0.5H, m), 3.92 (0.5H, s), 4.01 (0.5H, s), 4.67 (0.5H, dd, *J* = 6.7, 6.5 Hz), 4.78 (0.5H, dd, *J* = 5.2, 5.2 Hz), 5.45−5.48 (1H, m), 7.27−7.40 (5H, m), 8.50−8.61 (2H, m). ^{13}C NMR (DMSO-d_6, 125 MHz): δ (mixture of two diastereomers) 18.1, 25.0, 27.6, 28.1, 28.4, 29.5, 34.4, 42.2, 56.8, 56.8, 72.1, 72.2, 84.8, 127.9, 128.2, 128.9, 139.2, 139.4, 171.2, 171.4, 172.0. IR (KBr disk, cm^{-1}): 3297, 3071, 3041, 2967, 2938, 2535, 2124, 1734, 1653, 1527, 1456, 1427, 1375, 1299, 1199, 1137, 1070, 1027, 836. HRMS (ESI): $[M+Na]^+$ *m*/*z* calcd 440.1614, found 440.1626.

(4*S*)-2-(((*R*)-2-(Hex-5-ynamido)-2-(4-hydroxyphenyl)-acetamido)methyl)-5,5-dimethylthiazolidine-4-carboxylic Acid (10). Compound **10** was synthesized as described for compound **9** except that compound **8** was used instead of **7** (60 mg, 0.13 mmol). The product was purified by preparative HPLC (20−50% B over 25 min, 10 mL/min), and obtained as white powder (14.5 mg, 24%). ^{1}H NMR (DMSO-d_6, 500 MHz): δ (mixture of two diastereomers) 1.26 (3H, s), 1.55−1.59 (3H, pair of s), 1.61−1.67 (2H, m), 2.12−2.14 (2H, m), 2.24−2.27 (2H, m), 2.77 (1H, s), 3.20−3.26 (0.5H, m), 3.34−3.39 (0.5H, m), 3.42−3.47 (0.5H, m), 3.56−3.60 (0.5H, m), 4.03 (0.5H, s), 4.12 (0.5H, s), 4.68 (0.5H, dd, *J* = 6.5, 6.5 Hz), 4.79 (0.5H, dd, *J* = 5.5, 5.5 Hz), 5.28−5.31 (1H, m), 6.69 (2H, d, *J* = 8.5 Hz), 7.17 (2H, d, *J* = 8.5 Hz), 8.36−8.50 (3H, m). ^{13}C NMR (DMSO-d_6, 125 MHz): δ (mixture of two diastereomers) 17.5, 24.3, 26.9, 27.5, 27.7, 28.8, 33.8, 41.4, 55.7, 55.8, 71.4, 71.6, 84.2, 114.8, 115.0, 128.5, 128.7, 128.8, 156.9, 158.3, 158.6, 171.2, 171.3. IR (KBr disk, cm^{-1}): 3301, 3071, 3028, 2973, 2928, 2548, 2111, 1737, 1662, 1606, 1593, 1515, 1435, 1377, 1197, 1139, 837. HRMS (ESI): $[M+Na]^+$ *m*/*z* calcd 456.1564, found 456.1569.

Ent-Amp (11). Ampicillin-alkyne **7** (120 μL of an 80 mM solution in DMSO, 9.6 μmol) and Ent-PEG_3-N_3 **4** (250 μL of a 13 mM solution in 1,4-dioxane, 3.3 μmol) were combined, and 400 μL of DMSO was added. $CuSO_4$ (100 μL of a 90 mM solution in water, 9.0 μmol) and tris[(1-benzyl-1*H*-1,2,3-triazol-4-yl)methyl]amine (TBTA, 200 μL of a 50 mM solution in DMSO, 10 μmol) were combined, and 100 μL of DMSO was added to give a blue-green solution, to which NaAsc (400 μL of a 90 mM solution in water, 36.0 μmol) was added. This solution became light yellow and was immediately added to the alkyne/azide solution. The reaction was shaken on a benchtop rotator for 2 h at room temperature, diluted by 3- to 4-fold with 1:1 MeCN/water, centrifuged (13,000 rpm × 10 min, 4 °C), and purified by semi-

dx.doi.org/10.1021/ja503911p | *J. Am. Chem. Soc.* 2014, 136, 9677−9691

preparative HPLC (20% B for 5 min and 20%−50% B over 11 min, 4 mL/min; 0.005% TFA was used in the solvent system to prevent decomposition of the β-lactam). The HPLC fractions containing **11** were collected manually and flash frozen in liquid N_2 immediately after collection to prevent β-lactam decomposition. The product was obtained as white powder (3.3 mg, 76%). ^{1}H NMR (DMSO-d_6, 500 MHz): δ 1.40 (3H, s), 1.54 (3H, s), 1.78−1.81 (2H, m), 2.27 (2H, t, J = 6.8 Hz), 2.58 (2H, t, J = 6.5 Hz), 3.48 (12H, m), 3.76 (2H, s), 4.19 (1H, s), 4.38−4.44 (5H, m), 4.64−4.66 (3H, m), 4.91−4.92 (3H, m), 5.39 (1H, d, J = 3.5 Hz), 5.51−5.52 (1H, m), 5.72 (1H, d, J = 7.5 Hz), 6.74 (2H, dd, J = 7.8, 7.8 Hz), 6.96 (2H, d, J = 7.5 Hz), 7.26−7.35 (5H, m), 7.42−7.45 (3H, m), 7.81 (1H, s), 7.92 (1H, s), 8.33 (1H, s), 8.55 (1H, d, J = 7.5 Hz), 9.12 (3H, d, J = 7.0 Hz), 9.29 (1H, d, J = 6.5 Hz), 9.42 (2H, bs), 9.74 (1H, s), 11.6 (2H, s), 11.9 (1H, bs), 13.35 (1H, bs). HRMS (ESI): $[M+Na]^+$ m/z calcd 1379.4021, found 1379.4046.

Ent-Amx (12). Compound **12** was synthesized as described for **11** except that compound **8** was used instead of compound **7**. The product was obtained as white powder (2.9 mg, 66%). ^{1}H NMR (DMSO-d_6, 500 MHz): δ 1.40 (3H, s), 1.54 (3H, s), 1.78−1.80 (2H, m), 2.23 (2H, t, J = 6.5 Hz), 2.57 (2H, t, J = 6.5 Hz), 3.47 (12H, m), 3.76 (2H, bs), 4.18 (1H, s), 4.39−4.43 (5H, m), 4.63−4.65 (3H, m), 4.90 (3H, bs), 5.38 (1H, s), 5.52−5.56 (2H, m), 6.68 (2H, d, J = 8.5 Hz), 6.73 (2H, dd, J = 7.8, 7.8 Hz), 6.96 (2H, d, J = 7.5), 7.19 (2H, d, J = 8.5 Hz), 7.33 (2H, d, J = 7.5 Hz), 7.44 (1H, s), 7.80 (1H, s), 7.92 (1H, s), 8.33−8.39 (2H, m), 8.94 (1H, d, J = 8.0 Hz), 9.11−9.12 (2H, m), 9.29 (1H, bs), 9.38−9.43 (3H, m), 9.75 (1H, s), 11.6 (2H, bs), 11.9 (1H, bs). HRMS (ESI): $[M+Na]^+$ m/z calcd 1395.3970, found 1395.3982.

D-Ent-Amp (13). Compound **13** was synthesized as described for **11** except that compound **6** was used instead of compound **4**. The product was obtained as white powder (1.6 mg, 36%). HRMS (ESI): $[M+Na]^+$ m/z calcd 1379.4021, found 1379.4022.

D-Ent-Amx (14). Compound **14** was synthesized as described for **12** except that compound **6** was used instead of compound **4**. The product was obtained as white powder (2.9 mg, 66%). HRMS (ESI): $[M+Na]^+$ m/z calcd 1395.3970, found 1395.3995.

Ent-Hydro-Amp (15). Compound **15** was synthesized as described for **11** except that compound **9** was used instead of compound **7**. The product was obtained as white powder (1.8 mg, 21%). HRMS (ESI): $[M+H]^+$ m/z calcd 1331.4409, found 1331.4389.

Ent-Hydro-Amx (16). Compound **16** was synthesized as described for **12** except that compound **10** was used instead of compound **8**. The product was obtained as white powder (1.5 mg, 17%). HRMS (ESI): $[M+Na]^+$ m/z calcd 1369.4177, found 1369.4191.

General Procedures for Antimicrobial Activity Assays. General microbiology materials and methods, including details of Ent-Amp/Amx stock solution preparation and storage, are provided as Supporting Information. Overnight cultures of the bacterial strains (Table S1) were prepared in 15-mL polypropylene tubes by inoculating 5 mL of LB media with the appropriate freezer stock. The overnight cultures were incubated at 37 °C for 16−18 h in a tabletop incubator shaker set at 150 rpm and housing a beaker of water. Each overnight culture was diluted 1:100 into 5 mL of fresh LB media containing 200 μM 2,2′-dipyridyl (DP) and incubated at 37 °C with shaking at 150 rpm until OD_{600} reached 0.6. Each culture was subsequently diluted in 50% MHB medium (10.5 g/L) with or without 200 μM DP to achieve an OD_{600} value of 0.001. A 90-μL aliquot of the diluted culture was combined with a 10-μL aliquot of a 10× solution of the antibiotic or Ent-antibiotic conjugate in a 96-well plate, and the covered plate was wrapped in parafilm and incubated at 30 °C with shaking at 150 rpm for 19 h in a tabletop incubator housing a beaker of water. Bacterial growth was determined by measuring OD_{600} (end point analysis) using a BioTek Synergy HT plate reader. Each well condition was prepared in duplicate and at least three independent replicates using two different synthetic batches of each conjugate were conducted on different days. The resulting mean OD_{600} values are reported, and the error bars are the standard error of the mean (SEM) obtained from the independent replicates.

Antimicrobial Assays in the Presence of β-Lactamase Inhibitors. These assays were performed with *E. coli* ATCC 35218 and *K. pneumoniae* ATCC 13883 following the general procedure except that sulbactam (SB) or potassium clavulanate (PC) were mixed with ampicillin or amoxicillin and the Ent-Amp or Ent-Amx conjugates, respectively. The molar ratios of the inhibitor/β-lactam mixtures were sulbactam/Amp or Ent-Amp, 1.5:1, and potassium clavulanate/Amx or Ent-Amx, 0.9:1. These ratios were taken from the recipe of commercial drug combinations.[68] SB and PC were stored as DMSO stock solutions at −20 °C.

Antimicrobial Assays in the Presence of Exogenous Ent. These assays were performed with *E. coli* K-12 and CFT073 following the general procedure except that varying concentrations (1−100 μM) of synthetic L-Ent were mixed with Ent-Amp/Amx.

Antimicrobial Activity Assays in the Presence of Lipocalin 2. This assay is based on a published protocol[69] and was conducted with *E. coli* CFT073. Overnight cultures of *E. coli* CFT073 were grown in M9 minimal medium. Each overnight culture was serially diluted into M9 minimal medium to provide 10^3−10^4 CFU/mL. Lipocalin 2 was diluted in PBS to a concentration of 10 μM upon arrival, aliquoted, and stored at −20 °C until use. A 90-μL aliquot of the diluted culture was added to each well of a 96-well plate that contained varying concentrations of lipocalin 2, Ent-Amp, and Ent, and the final volume was adjusted to 100 μL with sterile PBS. The 96-well plate was incubated at 37 °C for 24 h in a tabletop incubator set at 150 rpm, and bacterial growth was determined by measuring OD_{600} using a plate reader. Each well condition was repeated at least three times independently on different days and with different batches of lipocalin 2. The resulting mean OD_{600} is reported, and the error bars are the SEM.

Time-Kill Kinetic Assays. A 5-mL overnight culture of *E. coli* K-12 or CFT073 was grown in LB (*vide supra*) and diluted 1:100 into 5 mL of fresh LB media containing 200 μM DP, and this culture was incubated at 37 °C with shaking at 150 rpm in a tabletop incubator housing a beaker of water until OD_{600} reached ∼0.3. The culture was centrifuged (3000 rpm × 10 min, rt), and the resulting pellet was washed twice by resuspension in 50% MHB and centrifugation (3000 rpm × 10 min, rt). The resulting pellet was resuspended in 50% MHB with or without DP, and the OD_{600} was adjusted to 0.3. A 90-μL aliquot of the resulting culture was mixed with a 10-μL aliquot of a 10× solution of Amp/Amx or the Ent-Amp/Amx in a 96-well plate, which was covered, wrapped in parafilm, and incubated at 37 °C with shaking at 150 rpm. The OD_{600} values were recorded at t = 0, 1, 2, and 3 h by using a plate reader. In a parallel experiment, a 10-μL aliquot of the culture was taken at t = 0, 1, 2, and 3 h, serially diluted by using sterile phosphate-buffered saline (PBS), and plated on LB-Agar plates for colony counting (CFU/mL). Each well condition was repeated at least three times independently on different days. The resulting mean OD_{600} or CFU/mL is reported, and the error bars are the SEM.

Mixed-Species Assays. A 5 mL overnight culture of each bacterial strain was grown in LB, diluted 1:100 into 5 mL of fresh LB media containing 200 μM DP, and incubated at 37 °C with shaking at 150 rpm in a tabletop incubator housing a beaker of water until OD_{600} reached 0.6. Each mid-log-phase culture was diluted to 10^6 CFU/mL in 50% MHB with or without 200 μM DP. For experiments requiring a mixture of two species, a 1:1 mixture was prepared (10^6 CFU/mL for each strain) in 50% MHB with or without 200 μM DP from the mid-log-phase cultures. To confirm CFU/mL of each culture, the single- and double-species cultures were serially diluted by using sterile PBS, and aliquots were plated on a CHROM-UTI plate ("starter-culture plate"). For each cell-killing experiment, a 90-μL aliquot of each culture was combined with a 10-μL aliquot of a 10 μM solution of the antibiotic or Ent-antibiotic conjugate in a 96-well plate, which was covered, wrapped in parafilm, and incubated at 30 °C with shaking at 150 rpm for 19 h. Bacterial growth was assayed both by measuring OD_{600} using the plate reader and by plating on CHROM-UTI plates after serial dilution ("assay plate"). Each well condition was repeated at least three times independently on different days. The resulting mean OD_{600} is reported, and the error bars are the SEM. Images of representative CHROM-UTI plates are presented.

Scheme 1. Syntheses of the L and D Forms of Ent-Amp/Amx

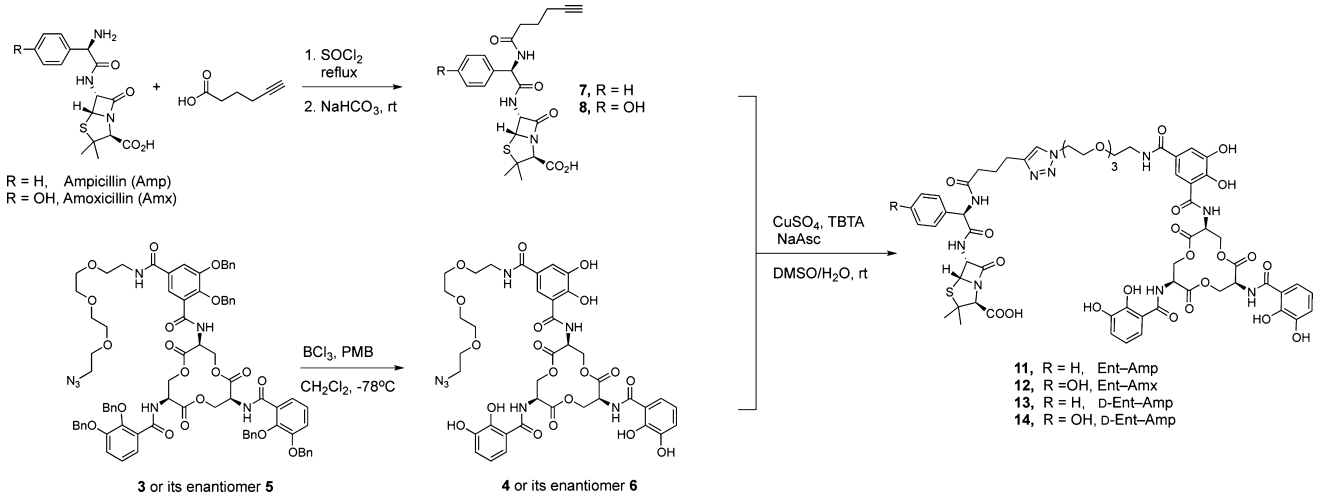

RESULTS AND DISCUSSION

Design and Syntheses of Enterobactin–Antibiotic Conjugates Harboring β-Lactams. We aimed to harness our enterobactin-mediated cargo delivery strategy to enable the transport of toxic cargo across the outer membrane of *E. coli*. To address this goal, we linked the β-lactam antibiotics ampicillin (Amp) and amoxicillin (Amx) to a monofunctionalized Ent scaffold where Ent is derivatized at the C5 position of one catechol ring via a flexible and stable PEG_3 linker. We selected Amp and Amx as antibacterial cargo for several reasons: these molecules are commercially available and amenable to synthetic modification, retain antibacterial activity when appropriately modified, possess periplasmic targets in Gram-negative bacteria and must cross the outer membrane to be active against these species, and have relatively low molecular weights. We selected low-molecular-weight antibiotics because our prior studies of Ent-mediated cargo transport indicated that the Ent transport machinery of *E. coli* K-12 imports Ent-cargo conjugates harboring relatively small cargos (e.g., cyclohexane, naphthalene, phenylmethylbenzene) to the cytosol readily, whereas large cargos (e.g., vancomycin) are not transported to the cytosol.[66] Moreover, in prior studies, various β-lactams including Amp and Amx have been linked to simple catechols[29−32,34−40] and more complex catechol-containing siderophores or mimics thereof,[43,44,49,50,53,56,70] which provides the opportunity to compare the outcomes obtained for different siderophore-inspired design strategies.

In Scheme 1, we present the syntheses of Ent-Amp **11** and Ent-Amx **12**, which feature installation of alkyne-modified β-lactam warheads onto Ent-azide **4** via copper-catalyzed azide-alkyne cycloaddition (hereafter click reaction) in the final step. The catechol moieties of benzyl-protected Ent-azide **3** were deprotected by using BCl_3 at −78 °C to achieve Ent-azide **4** as a white powder in 28% yield following purification by reverse-phase preparative HPLC. Catalytic hydrogenation using hydrogen gas and a Pd/C catalyst is typically employed to deprotect Ent catechols;[67,71] however, we observed that Amp/Amx decompose under these conditions and poison the Pd/C catalyst. Moreover, deprotection of the enterobactin catechols prior to installing the β-lactams requires preservation of the azide moiety, and we therefore employed BCl_3 for this reaction. Initial attempts at assembling Ent-Amp/Amx using standard conditions for the copper-catalyzed click reactions with Ent-azide **4** and the alkyne-modified β-lactams **7**/**8**, prepared by thionyl chloride coupling of 5-hexynoic acid to the amino group of Amp/Amx, failed because of copper-mediated β-lactam decomposition.[72] This problem was overcome by including the metal-ion chelator tris[(1-benzyl-1*H*-1,2,3-triazol-4-yl)methyl]-amine (TBTA)[73] in the click reactions, and Ent-Amp and Ent-Amx were obtained as white powders in high purity and yields of 66% and 76%, respectively, following semi-preparative HPLC purification. It was necessary to perform HPLC purification with eluents containing only 0.005% TFA to prevent decomposition of the acid-sensitive β-lactam moieties. This synthetic route was likewise employed to prepare the D-enantiomers of Ent-Amp/Amx **13** and **14** (Scheme 1).

This synthesis affords intermediates and reaction conditions of broad utility. Deprotected Ent-azide **4** enables alkyne-functionalized molecules to be covalently linked to Ent via a click reaction, including molecules that are incompatible with reaction conditions required to deprotect the Ent catechols. Moreover, the deprotected Ent-azide may be employed to append Ent to surfaces, other materials, or biomolecules harboring alkyne groups. This synthesis also provides opportunity to elaborate β-lactams for a variety of purposes. Indeed, very few examples employing the copper(I)-catalyzed click reaction with fused β-lactams are reported in the literature,[74,75] and it is likely that this paucity stems from the fact that β-lactams are incompatible with standard conditions for copper-catalyzed azide-alkyne cycloaddition.[72] The conditions defined in this work employing TBTA allow for copper-catalyzed triazole formation and preserve the β-lactam warhead.

Ent-Amp/Amx Coordinate Fe(III). In the absence of Fe(III), Ent-Amp/Amx exhibit an absorption band centered at 316 nm resulting from catecholate absorption and the solutions are colorless (MeOH, rt). Addition of 1.0 equiv of Fe(III) to methanolic solutions of Ent-Amp and Ent-Amx causes the solution to immediately change from colorless to purple-red, and a broad absorption feature in the 400−700 nm range appears (Figure S1), confirming that both Ent-Amp/Amx readily chelate Fe(III).

Ent-Amp/Amx Exhibit Enhanced Antibacterial Activity against Various *E. coli* Strains Including Human Pathogens. To ascertain whether Ent-Amp/Amx provide antibacterial activity against *E. coli*, including pathogenic strains,[76] we preformed antimicrobial activity assays using six

dx.doi.org/10.1021/ja503911p | J. Am. Chem. Soc. 2014, 136, 9677−9691

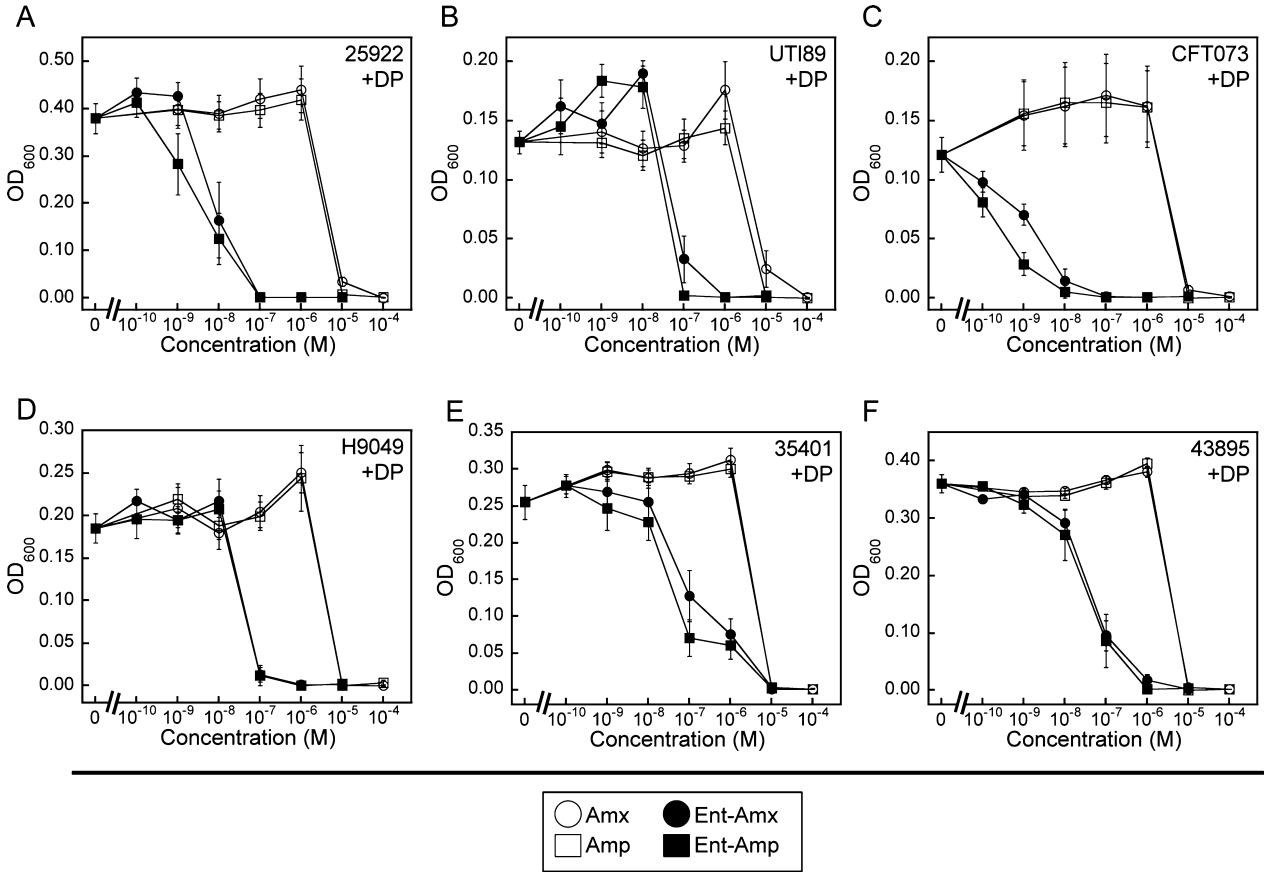

Figure 2. Antibacterial activity of Ent-Amp/Amx against various *E. coli* strains that include human pathogens. (A) Laboratory test strain *E. coli* ATCC 25922. (B) Uropathogenic *E. coli* UTI89. (C) Uropathogenic *E. coli* CFT073. (D) Non-pathogenic clinical isolate *E. coli* H9049. (E) Pathogenic ETEC *E. coli* ATCC 35401. (F) Pathogenic EHEC *E. coli* ATCC 43895. All assays were performed in 50% MHB medium supplemented with 200 μM DP to provide iron-limiting conditions (mean ± SEM, $n \geq 3$). The data for assays performed in the absence of DP are presented in Figures S2−S7.

strains (Table S1, Figures 2, S2−S7). *E. coli* ATCC 25922 is a laboratory susceptibility test strain originally obtained as a clinical isolate. *E. coli* H9049 is a non-pathogenic clinical isolate.[77] *E. coli* UTI89[78] and CFT073[79] are both pathogens of the human urinary tract (UPEC).[80] *E. coli* ATCC 35401 (serotype O78:H11) is an enterotoxigenic (ETEC) strain that was isolated from human feces. *E. coli* ATCC 43895 (serotype O157:H7) is an enterohemorrhagic (EHEC) strain that was isolated from raw hamburger meat implicated in a hemorrhagic colitis outbreak. Both ETEC and EHEC strains produce virulence factors and toxins and cause diarrhea in humans.[76] All *E. coli* strains biosynthesize Ent for iron acquisition and express the Ent receptor FepA. Some *E. coli* strains employed in this work also have the capacity to produce and utilize salmochelins, C-glucoyslated Ent derivatives.[81] These molecules are produced by *Salmonella* spp. and pathogenic *E. coli* strains for iron acquisition. The *iroA* gene cluster (*iroBCDEN*) encodes proteins required for the biosynthesis and transport of salmochelins, and IroN is the outer membrane receptor for salmochelins encoded by the *iroA* cluster.[82,83] Studies with *Salmonella* indicate that IroN has the ability to transport Ent as well as its glucosylated forms.[84] Of the strains considered in this work, *E. coli* CFT073 and UTI89 harbor the *iroA* gene cluster. *E. coli* H9049 does not produce salmochelins,[85] and a BLAST search using available *E. coli* genomes reveals that the *E. coli* 43985 genome does not contain the *iroA* cluster. The genome for *E. coli* ATCC 25922 is unpublished; however, this strain is reported to be sensitive to lipocalin-2 (*vide infra*),[86] which suggests that its genome does not encode the *iroA* cluster. Whether *E. coli* 35401 produces salmochelins is unclear from the available literature. Lastly, it should be noted that *E. coli* CFT073 is celebrated for having redundant iron import machineries, and this strain also harbors the *iha* gene, which encodes the outer membrane Ent receptor Iha that is distinct from FepA.[87]

We performed antibacterial activity assays using a 10-fold dilution series to compare the abilities of Ent-Amp/Amx and unmodified Amp/Amx to kill *E. coli* (Figures 2, S2−S7). These assays were conducted in 50% MHB and in the absence or presence of 200 μM DP. The latter growth conditions provide iron limitation and result in expression of the Ent uptake machinery FepABCDG. Amp/Amx exhibit minimum inhibitory concentration (MIC) values of 10 μM against these *E. coli* strains regardless of the presence of DP in the growth medium (Figures 2, S2−S7). All six *E. coli* strains are more susceptible to Ent-Amp/Amx than Amp/Amx under conditions of iron limitation (Figure 2). Based on the 10-fold dilution series, Ent-Amp/Amx are 100-fold more potent against *E. coli* 25922, UTI89, and H9049 under iron-limiting conditions. Although the MIC values for 35401 and 43895 are only ca. 10-fold higher than for Amp/Amx in this assay, a significant reduction in growth is observed at 100 nM Ent-Amp/Amx, whereas this concentration of Amp/Amx affords no growth inhibition. The enhanced sensitivity of *E. coli* CFT073 to Ent-Amp/Amx is

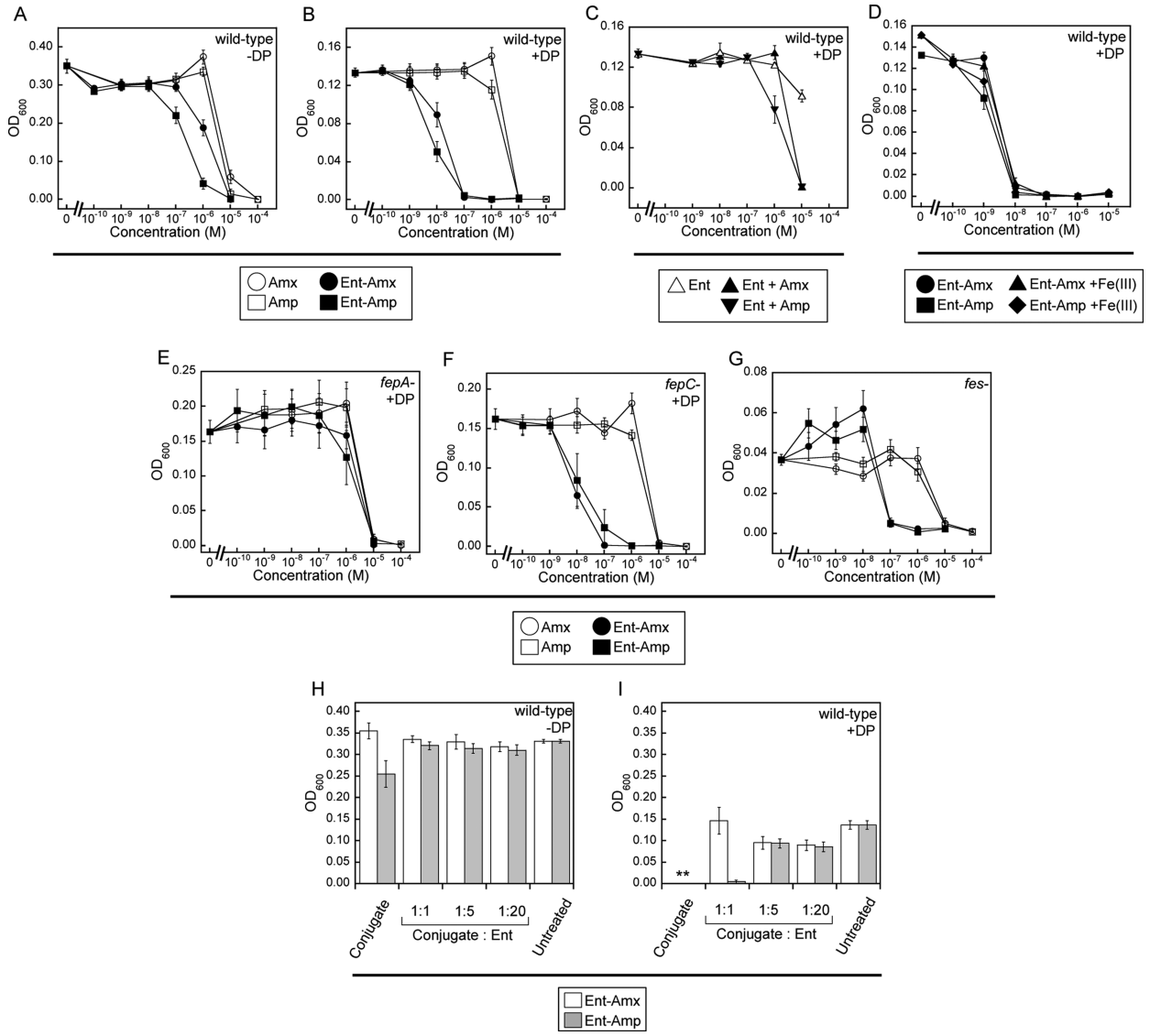

Figure 3. Antibacterial activity of Ent-Amp/Amx against wild-type and mutant *E. coli* K-12. (A,B) Growth inhibition of *E. coli* K-12 by Amp/Amx and Ent-Amp/Amx in the absence (A) and presence (B) of DP. (C) Growth inhibition of *E. coli* K-12 treated with a 1:1 molar ratio of Ent/Amp and Ent/Amx. (D) Growth inhibition of *E. coli* K-12 treated with ferric Ent-Amp/Amx. (E–G) Growth inhibition of *fepA-* (E), *fepC-* (F), and *fes-* (G) by Amp/Amx and Ent-Amp/Amx. (H,I) Growth of *E. coli* K-12 in the presence of 1 μM Ent-Amp/Amx ("conjugate") and mixtures of Ent-Amp/Amx (1 μM) and 1, 5, or 20 equiv of exogenous Ent in the absence (H) and presence (I) of DP. The ** indicates $OD_{600} < 0.01$. All assays were performed in 50% MHB medium with or without 200 μM DP (see panels) (mean ± SEM, $n \geq 3$). The data for additional assays performed in the absence of DP are presented in Figure S8.

remarkable. This strain exhibits the greatest sensitivity to Ent-Amp/Amx, providing a 1000-fold decreased MIC value (10 nM), and growth inhibition in the presence of ≤1 nM of the conjugate. Moreover, in the absence of DP, *E. coli* CFT073 exhibits the greatest susceptibility to Ent-Amp/Amx (Figures S2–S7). A noteworthy characteristic of CFT073 is its multiple mechanisms for iron acquisition, and we hypothesize that the presence of multiple receptors that recognize and transport Ent (FepA, IroN, Iha) contributes to this enhanced sensitivity. CFT073 and UTI89 both express IroN, which may indicate that Iha is responsible for the enhanced susceptibility of CFT073; however, we cannot rule out the possibility that the conserved receptors function differently or exhibit different expression levels depending on the strain. Moreover, other unappreciated mechanisms may contribute to the potent bactericidal action exhibited by Ent-Amp/Amx against CFT073 and other strains.

Ent-Amp/Amx Exhibit Enhanced Antimicrobial Activity against *E. coli* K-12. To gain further insight into the mechanism of Ent-Amp/Amx antibacterial action, we performed a series of experiments with the standard laboratory strain *E. coli* K-12. We employed the same 10-fold dilution series to compare the activities of Ent-Amp/Amx and Amp/Amx against K-12. In the absence of DP, Ent-Amp/Amx and Amp/Amx exhibit comparable MIC values, with complete killing observed at ∼10 μM. At lower concentrations, Ent-Amp/Amx exhibit slightly greater antibacterial activity than unmodified Amp/Amx (Figure 3A). This phenomenon is most evident at a conjugate/drug concentration of 1 μM, where Ent-Amp/Amx inhibit *E. coli* K-12 growth to varying degrees and Amp/Amx do not affect bacterial growth. Under conditions of

dx.doi.org/10.1021/ja503911p | *J. Am. Chem. Soc.* 2014, 136, 9677–9691

iron limitation, a 100-fold reduction in MIC value (10 μM to 100 nM) for Ent-Amp/Amx is observed, and ca. 50% growth inhibition occurs at 10 nM of each conjugate (Figure 3B). These trends are comparable to those observed for *E. coli* ATCC 25922, H9049, and UTI89 (Figures 2, S2, S3, and S5). When the antibacterial activity assay was performed using a 1:1 ratio of native L-Ent and Amp/Amx, no reduction of Amp/Amx MIC values was observed (Figure 3C), which suggests the conjugation between Ent and the β-lactams is required for the enhanced bactericidal action. Moreover, treatment of *E. coli* K-12 with the iron-bound forms of Ent-Amp/Amx, obtained by pre-incubating each conjugate with 1 equiv of ferric chloride, afforded the same MIC values as observed for apo Ent-Amp/Amx. These results indicate that the enhanced antibacterial activity does not result from iron chelation in the growth media (Figure 3D). In total, the data obtained for *E. coli* K-12 as well as the six other *E. coli* strains demonstrate that the antibacterial activity of Ent-Amp/Amx against *E. coli* K-12 is enhanced under conditions of iron limitation and support a model of Ent-mediated delivery of antibacterial cargo to the *E. coli* periplasm.

FepA Is Essential for Ent-Amp/Amx Antimicrobial Activity against *E. coli* K-12. To evaluate transport of Ent-Amp/Amx into *E. coli*, we investigated the antimicrobial activity of Ent-Amp/Amx and Amp/Amx against three single-gene knockout *E. coli* K-12 strains obtained from the Keio Collection,[88] *fepA-*, *fepC-*, and *fes-* (Figures 3E–G and S8). We selected these mutants to ascertain how components of the enterobactin transport and processing machinery contribute to Ent-Amp/Amx antibacterial activity. *E. coli fepA-* lacks the outer membrane Ent receptor FepA that allows periplasmic delivery, *fepC-* lacks the ATPase component of the inner membrane Ent permease that transports Ent into the cytosol, and *E. coli fes-* lacks the cytoplasmic esterase Fes responsible for hydrolysis of the Ent macrolactone for iron release. On the basis of our studies with wild-type K-12 and other *E. coli* strains, we hypothesized that the activity of Ent-Amp/Amx would be attenuated for the *fepA-* mutant. Moreover, we questioned whether loss of FepC or Fes would modulate the antimicrobial activity.

Overnight cultures of *fepA-* and *fepC-* reached OD_{600} values (~0.15) similar to that observed for wild-type K-12 when grown in 50% MHB supplemented with 200 μM DP. In contrast, the *fes-* strain exhibited a severe growth defect under these conditions ($OD_{600} \approx 0.04$). Treatment of *fepA-* with Ent-Amp/Amx afforded the same MIC values as for Amp/Amx (Figure 3E) and hence a 100-fold reduction in activity as compared to wild-type K-12. Iron deprivation is deleterious to *E. coli*, and we contend that the growth inhibition observed at 10 μM Ent-Amp/Amx results from iron starvation rather than an antibacterial activity of the Amp/Amx cargo. Analysis of 50% MHB by inductively coupled plasma optical emission spectroscopy (ICP-OES) revealed a total iron concentration of ca. 4 μM (Table S2), which can be compared to 10 μM of a high-affinity extracellular iron chelator. Indeed, we previously observed similar growth inhibition of *fepA-* with 10 μM of an Ent-vancomycin conjugate (extracellular iron chelation) and also 10 μM D-Ent (iron chelator that cannot be used for iron acquisition) under these growth conditions.[66] These data confirm that FepA is essential for the potent antibacterial activity of Ent-Amp/Amx against *E. coli* K-12.

In contrast to *fepA-*, the growth of *fepC-* and *fes-* was completely inhibited with 100 nM Ent-Amp/Amx under iron-limiting conditions (Figure 3F,G), comparable to what was observed for the wild-type strain. The targets of β-lactam antibiotics are penicillin binding proteins (PBPs), which are located in the periplasm of Gram-negative bacteria. After crossing the outer membrane through FepA, Ent-Amp/Amx enter the periplasm where covalent capture by the PBPs presumably occurs. Thus, it is reasonable that the downstream Ent transport and processing steps involving FepCDG and Fes do not affect the antimicrobial activity of the conjugates if they are trapped in the periplasm as a result of PBP binding. Although it is possible that the Ent uptake machinery (e.g., periplasmic binding protein FepB) competes with the PBPs for Ent-Amp/Amx, no improved antibacterial activities were observed for the *fepC-* and *fes-* mutants compared to wild-type K-12. This observation indicates that Ent-Amp/Amx bind to PBPs and are trapped in the periplasm. It should be noted that the *fepB-* mutant, which lacks the periplasmic binding protein, was also considered in this work; however, this strain exhibited a severe growth defect and afforded inconsistent results.

Ent-Amp/Amx and L-Ent Compete for FepA Recognition. To probe interaction between FepA and Ent-Amp/Amx, we performed growth inhibition assays employing mixtures of Ent-Amp/Amx and varying concentrations of unmodified Ent (Figure 3H–I). When these assays were performed under conditions of iron limitation, the presence of exogenous Ent attenuated the antibacterial activity of Ent-Amp/Amx. A 1:1 molar ratio of Ent-Amx/Ent afforded an OD_{600} value comparable to that of the untreated control, whereas higher equivalents of Ent were required to block the antibacterial action of Ent-Amp. The origins of this difference are unclear and may indicate that the hydroxyl group of Amx has a negative effect on the transport efficiency of the conjugate. In total, these Ent addition assays suggest that competition for Ent-Amp/Amx and Ent occurs at the receptor(s) and that the conjugates are delivered into the bacteria via the same uptake machinery as Ent.

Antibacterial Activity of D-Ent-Amp/Amx. L-Serine is a biosynthetic building block for Ent, and a role for chiral recognition in Ent transport has been probed in prior studies.[89,90] In one series of investigations, *E. coli* FepA was found to bind ferric L-Ent and ferric D-Ent with similar affinities (K_d = 21 and 17 nM, respectively; ascertained by measuring the binding of ^{59}Fe-loaded siderophores to *E. coli* BN1071 cells).[89] A lack of transport of ferric D-Ent into *E. coli* BN1071 was also reported in this work. A later study probed Ent uptake in *Bacillus subtilis*, and transport of both L- and D-Ent analogues was observed to occur with similar efficiency.[90] Moreover, the ability of Fes from *Shigella flexneri* 2a str. 2457T to hydrolyze L-Ent and D-Ent was evaluated, and Fes did not accept D-Ent as a substrate. As a result of the transport studies in *B. subtilis* and enzymatic activity assays with *S. flexneri* Fes, a model in which both Ent enantiomers are transported and chiral recognition occurs at the level of the esterase was proposed.[90] Taken together, these studies suggest that the ability to transport D-Ent may vary between species and even between strains of a given species, and more studies are required to address such possibilities. Based on the observation that *E. coli* FepA binds D-Ent and that *B. subtilis* transports D-Ent analogues, we synthesized the D-enantiomers of the Ent-β-lactam conjugates (**13** and **14**, Scheme 1) and evaluated the antibacterial activity of these conjugates against *E. coli* K-12, 25922, CFT073, 35401, and 43895 (Figures S9–S13). D-Ent-Amp/Amx exhibited reduced antibacterial activity relative to Ent-Amp/Amx for K-

dx.doi.org/10.1021/ja503911p | J. Am. Chem. Soc. 2014, 136, 9677–9691

Scheme 2. Syntheses of Ent-Hydro-Amp/Amx

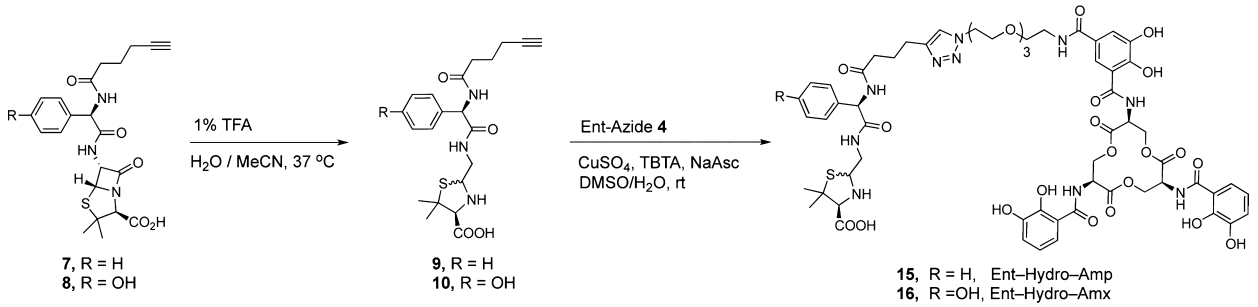

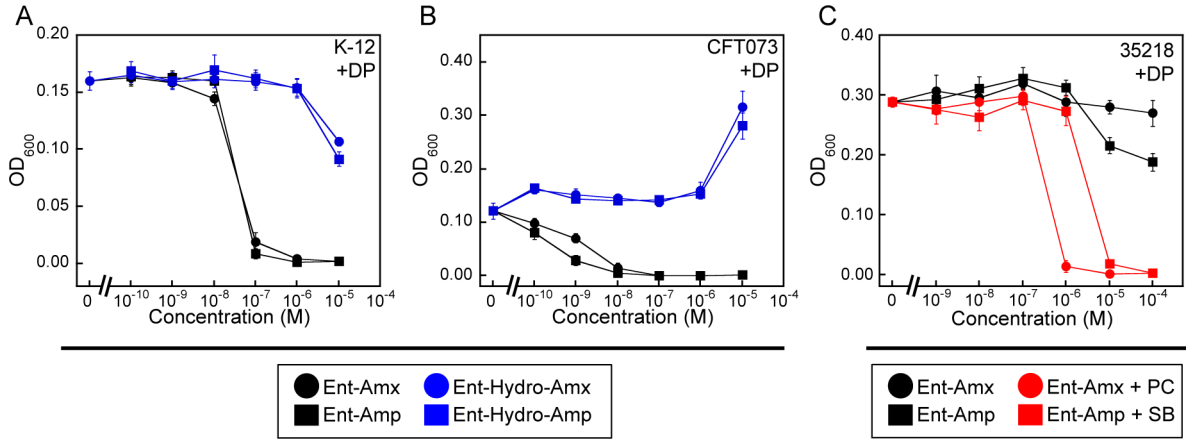

Figure 4. β-Lactam is required for Ent-Amp/Amx antimicrobial activity. (A,B) Antibacterial activity assays against *E. coli* K-12 (A) and CFT073 (B) using Ent-Amp/Amx and Ent-Hydro-Amp/Amx. (C) Antibacterial activity assays against *E. coli* ATCC 35218, which expresses a class A serine β-lactamase, using Ent-Amp/Amx in the absence and presence of the β-lactamase inhibitors potassium clavulanate (PC) and sulbactam (SB). All assays were performed in 50% MHB supplemented with 200 μM DP (mean $\pm$ SEM, $n \geq 3$). Additional data are presented in Figure S14.

12, 25922, CFT073, and 43895. Under conditions of iron limitation, complete growth inhibition was observed with 1 μM D-Ent-Amp/Amx for *E. coli* K-12, 25922, and 43895, compared to 100 nM for Ent-Amp/Amx. Likewise, a 10-fold reduction in antibacterial activity was observed for *E. coli* CFT073, where 100 nM D-Ent was required to inhibit growth completely. In contrast, a negligible difference in antibacterial activity of the L- and D-isomers was observed for *E. coli* 35401. Regardless of enantiomer, all four Ent-Amp/Amx conjugates provide enhanced antibacterial activity against these *E. coli* strains relative to Amp/Amx. Nevertheless, these data suggest that D-Ent-Amp/Amx are less readily transported into various *E. coli* strains than the L-isomers. Although this modification provides no appreciable benefit for this β-lactam delivery system with periplasmic targets, it is possible that Ent-antibiotic conjugates based on D-Ent may be desirable for delivering cargos to the cytosol, precluding concomitant delivery of nutrient Fe(III).

The Ent-Amp/Amx β-Lactam Warhead Is Essential for Antimicrobial Activity. With support for Ent-mediated delivery of Ent-Amp/Amx to the *E. coli* periplasm, we sought to confirm the essentiality of the β-lactam warheads in antibacterial action. We therefore designed and prepared hydrolyzed Ent-Amp/Amx analogues **15** and **16** (Scheme 2) where the β-lactam structure is destroyed. Hydrolysis of the Amp/Amx-alkynes **7** and **8** was achieved in the presence of 1% TFA with heating at 37 °C, and the decomposition products **9** and **10** were obtained as diastereomeric mixtures (Scheme 2). The formation of these species followed the reported degradation pathways for ampicillin, where hydrolysis and subsequent decarboxylation occur.[91] The diastereomeric mixtures were employed to prepare the hydrolyzed conjugates Ent-Hydro-Amp **15** and Ent-Hydro-Amx **16** via a copper-catalyzed click reaction.

We employed Ent-Hydro-Amp/Amx in antibacterial activity assays against *E. coli* K-12 and observed negligible growth inhibition (Figure 4A). When *E. coli* CFT073 was treated with Ent-Hydro-Amp/Amx in the presence of DP, growth recovery occurred at micromolar concentrations (Figure 4B). This result indicates that Ent-Hydro-Amp/Amx are transported into the cytoplasm of *E. coli* CFT073, where nutrient iron is released.

We also performed a series of antibacterial activity assays with *E. coli* ATCC 35218, a strain that expresses a class A serine β-lactamase. Similar to unmodified Amp/Amx, Ent-Amp/Amx were inactive against *E. coli* ATCC 35218 (MIC > 10 μM) in the absence and presence of DP (Figures 4C and S14). Slight growth inhibition was observed at 10 μM under conditions of iron limitation, which may be attributed to iron chelation. The addition of β-lactamase inhibitors restored the activities of Ent-Amp/Amx and Amp/Amx, and the conjugates exhibited greater antibacterial activity than the parent antibiotics (Figures 4C and S14). In total, the assays with Ent-Hydro-Amp/Amx and strains expressing β-lactamase demonstrate that an intact β-lactam is required for the antibacterial activity of Ent-Amp/Amx. Moreover, these studies indicate that the β-lactams retain their original function and inhibit PBPs when conjugated to Ent.

Time-Kill Kinetics Reveal Rapid Killing of *E. coli* CFT073 by Ent-Amp/Amx. The remarkable sensitivity of *E.*

dx.doi.org/10.1021/ja503911p | J. Am. Chem. Soc. 2014, 136, 9677−9691

coli CFT073 to Ent-Amp/Amx (Figure 2C) motivated us to investigate the relative cell-killing kinetics of Ent-Amp/Amx and Amp/Amx to determine whether these conjugates kill *E. coli* CFT073 more rapidly than the unmodified drugs. For comparison between *E. coli* strains, we also evaluated the time-kill kinetics for *E. coli* K-12. Ent-Amp/Amx provide more rapid cell death than unmodified Amp/Amx (Figure 5), and this

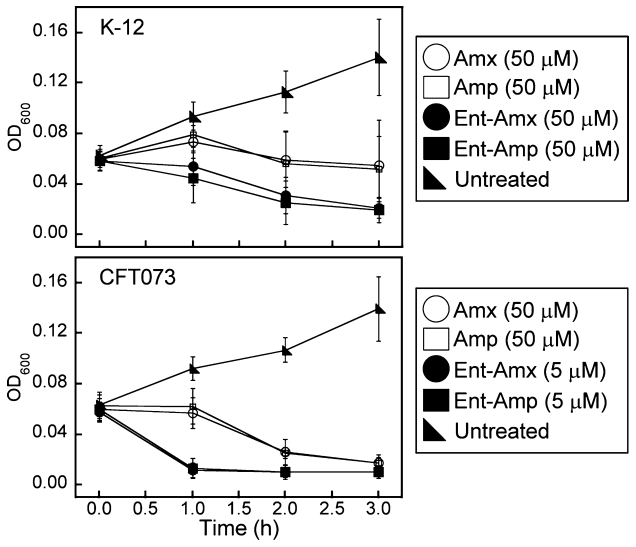

Figure 5. Time-kill kinetic assays for treatment of *E. coli* K-12 (top panel) and CFT073 (bottom panel) with Amp/Amx and Ent-Amp/Amx. *E. coli* K-12 (~10^8 CFU/mL) was treated with 50 μM of Amp/Amx or 50 μM Ent-Amp/Amx. *E. coli* CFT073 (~10^8 CFU/mL) was treated with 50 μM of Amp/Amx or 5 μM Ent-Amp/Amx. The assays were conducted in 50% MHB medium containing 200 μM DP at 37 °C (mean ± SEM, n = 3).

behavior is most apparent for *E. coli* CFT073, where the OD_{600} value was almost reduced to the baseline value after 1 h incubation with 5 μM Ent-Amp/Amx, corresponding to a 2-fold log reduction in CFU/mL. In contrast, the change in OD_{600} and CFU/mL for *E. coli* CFT073 treated with 50 μM unmodified Amp/Amx is negligible over this time period. The time-kill kinetics for *E. coli* K-12, conducted with 50 μM of both unmodified and modified β-lactams, indicate a slight increase in kill kinetics for Ent-Amp/Amx relative to Amp/Amx, and that the kinetics of cell-killing are slower for K-12 than CFT073 (Figure 5). These results support a model whereby Ent modification facilitates uptake of Amp/Amx relative to the unmodified drugs. This effect is more dramatic for *E. coli* CFT073 than K-12, which is in accordance with the enhanced antibacterial activity observed for CFT073 relative to the other *E. coli* strains considered in this work.

Ent-Amp/Amx Provides Species-Selective Antimicrobial Activity. To determine whether Ent-Amp/Amx exhibit broad-spectrum or species-selective activity, we performed antibacterial activity assays with two additional Gram-negative and two Gram-positive species in both the absence and presence of DP. These species include *Klebsiella pneumoniae* ATCC 13883, *Pseudomonas aeruginosa* PAO1, *S. aureus* ATCC 25923, and *Bacillus cereus* ATCC 14579. *K. pneumoniae* is a Gram-negative species that biosynthesizes and utilizes Ent for iron acquisition. *P. aeruginosa* is a Gram-negative bacterium that captures Ent as a xenosiderophore and expresses two Ent receptors PfeA and PirA.[92−94] *S. aureus* and *B. cereus* are both Gram-positive bacterial species, and the ability to utilize ferric Ent as an iron source is reported for both species.[95,96] In contrast to Gram-negative bacteria, where the PBPs are located in the periplasm, the targets of β-lactam antibiotics are in the extracellular peptidoglycan of Gram-positive organisms.

K. pneumoniae ATCC 13883 has a chromosomally encoded class A β-lactamase (SHV-1) and lacks sensitivity to Amp/Amx. We observed no effect of 100 μM Amp/Amx on *K. pneumoniae* growth under our assay conditions (Figure S15). Only ~50% growth inhibition was observed when *K. pneumoniae* was treated with high concentrations (10 μM) of Ent-Amp/Amx in the absence of DP, and the Ent-Amp conjugate provided the greatest activity under conditions of iron limitation with ~90% growth inhibition at 10 μM. When β-lactamase inhibitors were included in the assays, *K. pneumoniae* exhibited greater sensitivity to Amp/Amx (MIC = 100 μM) and Ent-Amp/Amx (MIC = 10 μM); however, we observed some growth inhibitory activity of the β-lactamase inhibitor sulbactam alone under these assay conditions (100 μM SB, Figure S15). Thus, the possibility of a synergistic effect from the inhibitors and conjugates cannot be ruled out completely. The lack of activity of Ent-Amp/Amx against *K. pneumoniae* ATCC 13883 is reminiscent of results obtained during investigations of Amp/Amx-functionalized tripodal triscatecholate ligands.[53] These compounds were inactive against *K. pneumoniae*, and the behavior was attributed to either an inability of the *K. pneumoniae* iron transport machinery to import the conjugates or the development of resistance over the course of the assay. An alternative explanation is that β-lactamase expression by *K. pneumoniae* resulted in inactivation of the β-lactams.

The *P. aeruginosa* PAO1 strain employed in this work exhibited little sensitivity to both Amp/Amx and the conjugates under the antibacterial assay conditions (Figure S16). Amp/Amx exhibited no activity up to 100 μM, whereas Ent-Amp/Amx provided growth inhibition at 10 μM in both the absence and presence of DP. Whether these results indicate that Ent-Amp/Amx will be ineffective against multiple *P. aeruginosa* strains is unclear. *P. aeruginosa* strains exhibit different phenotypes, and highly variable and strain-dependent MIC values have been reported for triscatecholate−β-lactam conjugates against *P. aeruginosa*.[53] We previously reported that *P. aeruginosa* PAO1 imports Ent-cargo conjugates,[66] and we speculate that the lack of activity observed for this strain stems from its inherent insensitivity to Amp/Amx.

B. cereus ATCC 14579 was also insensitive to Amp/Amx, which only afforded growth inhibition at 100 μM. Some growth inhibition was observed for *B. cereus* treated with 10 μM Ent-Amp/Amx, which may result from iron sequestration (Figure S17). *S. aureus* ATCC 25923 is susceptible to Amp/Amx, with complete growth inhibition observed at 1 μM. In this case, a 10-fold reduction in antibacterial activity was observed for Ent-Amp/Amx relative to unmodified Amp/Amx (Figure 6). Although the origins of this attenuation are unclear, we speculate that Ent-Amp/Amx may have trouble penetrating the thick peptidoglycan of *S. aureus*. An alternative possibility is that recognition of Ent-Amp/Amx by the *S. aureus* Ent receptor diverts the β-lactams from the PBPs.

In total, the results from these assays indicate that Ent-Amp/Amx exhibit antibacterial activity enhancements that are species-selective, providing increased potency against *E. coli* strains and not for the other strains evaluated in this work. We therefore reasoned that Ent-Amp/Amx, at low concentrations,

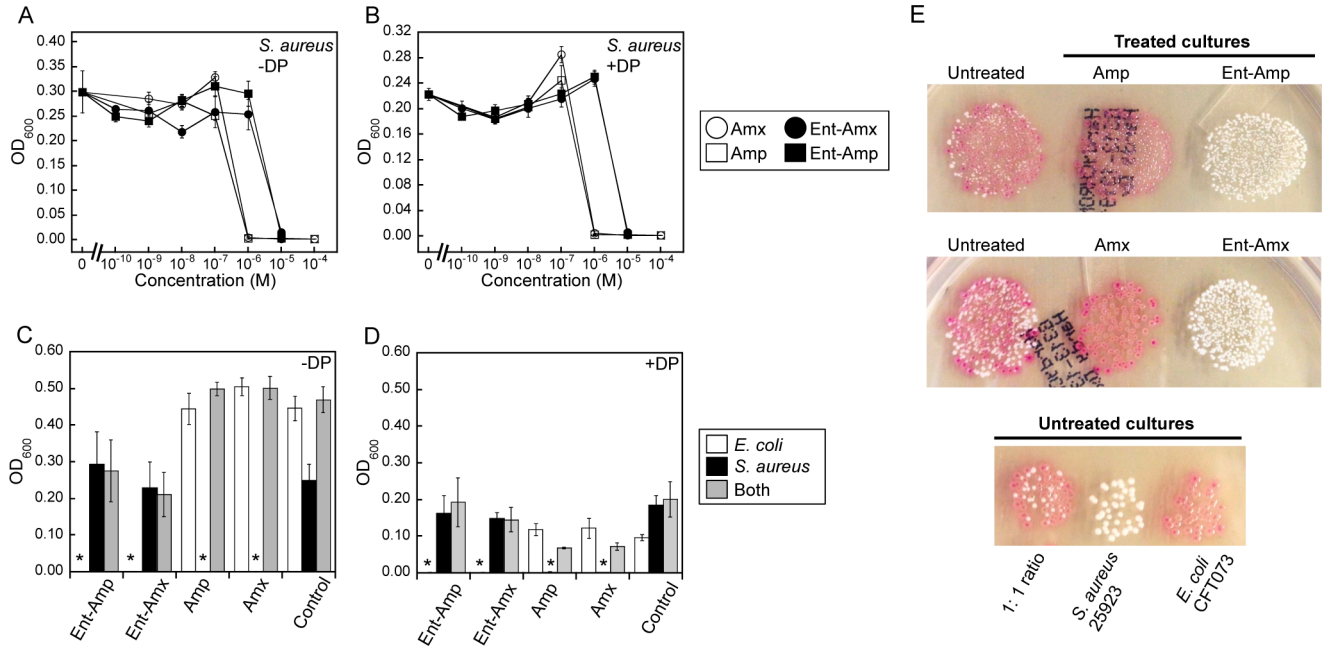

Figure 6. Ent-Amp/Amx selectively kill *E. coli* CFT073 in the presence of *S. aureus* ATCC 25923. (A,B) Antimicrobial activity assays against *S. aureus* ATCC 25923 in the absence (A) and presence (B) of 200 μM DP. (C,D) Bacterial growth monitored by OD_{600} for cultures of *E. coli* only, *S. aureus* only, and 1:1 *E. coli*/*S. aureus* mixtures treated with Amp/Amx or Ent-Amp/Amx in the absence (C) and presence (D) of 200 μM DP. The * indicates $OD_{600} < 0.01$. (E) Representative photographs of colonies from mixed cultures of *E. coli* CFT073 and *S. aureus* ATCC 29523 treated with Ent-Amp/Amx (1 μM) or Amp/Amx (1 μM) in the presence of 200 μM DP. All assays were conducted in 50% MHB medium (t = 19 h, 30 °C) (mean ± SEM, $n \geq 3$ for A–D).

should selectively kill *E. coli* in the presence of other less sensitive species. We treated co-cultures of *E. coli* CFT073 and *S. aureus* with Ent-Amp/Amx or Amp/Amx and analyzed the species composition following a 19-h incubation using HARTY-UTI plates. These agar plates are employed in medical microbiology laboratories for the diagnosis of urinary tract infections and provide species identification by the colony color. When grown on HARTY-UTI plates, *S. aureus* are off-white and *E. coli* are purple-pink. In Figure 6, we present representative images of the colonies that resulted from treating co-cultures of *E. coli* and *S. aureus* with Amp/Amx or Ent-Amp/Amx. In the absence of antibiotic, the cultures provide a mixture of off-white and purple-pink colonies, indicating that both *E. coli* and *S. aureus* grow when cultured together. When the co-cultures are treated with 1 μM Amp/Amx, only purple-pink colonies are present, which reveals that only *E. coli* survives. In contrast, treatment of the co-cultures with 1 μM Ent-Amp/Amx results in only off-white colonies from *S. aureus*. These comparisons demonstrate that Ent-Amp/Amx selectively kill *E. coli* in the presence of *S. aureus* and that the siderophore modification reverses the inherent species selectivity of the parent antibiotics. Achieving such species-selective and single-pathogen antibiotic targeting is an important goal and unmet need for pharmaceutical development that will allow for treating disease with minimal perturbation to the commensal microbiota.[97,98]

Ent-Amp Exhibits Low Cytotoxicity to Mammalian Cells. We evaluated the cytotoxicity of Ent-Amp against the human T84 colon epithelial cell line. Cell survival was evaluated by MTT assay after a 24 h treatment with apo or iron-bound Ent-Amp, Amp, or Ent. The iron-bound forms were assayed to determine whether iron chelation in the growth medium is a factor. No cytoxicity was observed for Amp or Ent-Amp, whereas apo Ent itself decreased the survival of T84 cells by approximately 30% at the highest concentration evaluated. When pre-loaded with Fe(III), no cytotoxic effect from Ent was observed (Figure 7).

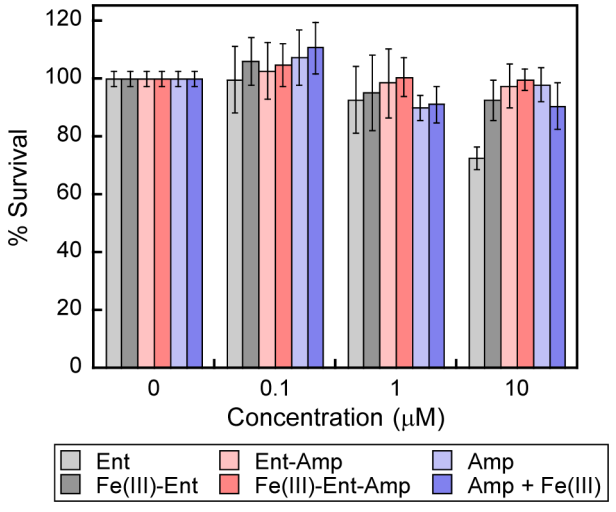

Figure 7. Ent-Amp exhibit negligible cytotoxicity toward human T84 intestinal epithelial cells. Percent cell survival quantified by MTT assay after a 24 h treatment with apo or iron-bound Ent, Ent-Amp, and the parent antibiotic Amp in the absence and presence of 1 equiv of Fe(III) (mean ± SEM, n = 3).

FepA and Lipocalin-2 Compete for Ent-Amp/Amx. Lipocalin-2 (lcn2, also known as siderocalin or NGAL) is a 22-kDa protein produced and released by neutrophils and epithelial cells. It has a hydrophobic binding pocket and coordinates ferric Ent with sub-nanomolar affinity.[69,85] By sequestering ferric Ent, this host-defense protein contributes to

dx.doi.org/10.1021/ja503911p | J. Am. Chem. Soc. 2014, 136, 9677–9691

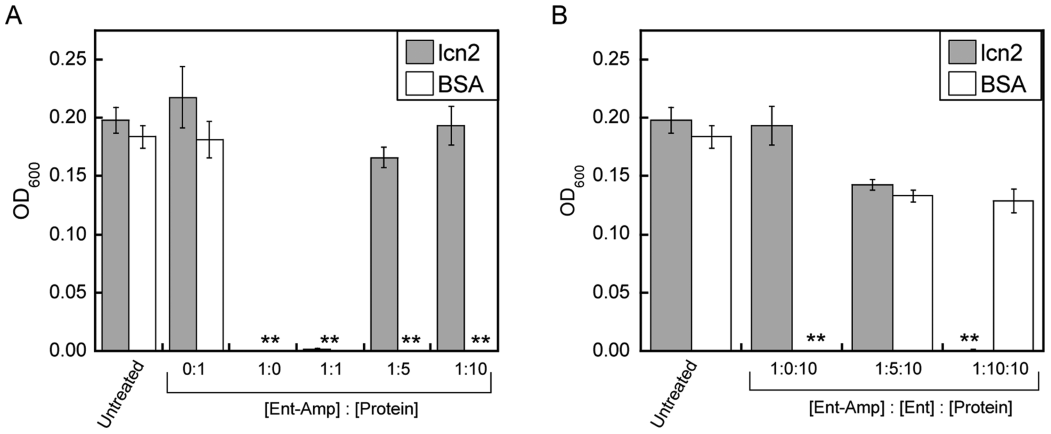

Figure 8. Antibacterial activity of Ent-Amp against *E. coli* CFT073 in the presence of lcn2 or BSA. (A) *E. coli* CFT073 treated with 100 nM Ent-Amp and varying concentrations of lcn2 or BSA control. (B) *E. coli* CFT073 treated with Ent-Amp, varying concentration of Ent, and varying concentrations of lcn2 or BSA control. The assays were performed in M9 minimal medium (24 h, 37 °C) (mean ± SEM, $n \geq 3$). The ** indicates $OD_{600} < 0.01$.

the metal-withholding response and prevents bacterial acquisition of this essential nutrient. To determine whether lcn2 also binds Ent-Amp/Amx and thereby blocks antibacterial activity, we performed antibacterial activity assays with *E. coli* CFT073 in M9 minimal medium supplemented with lcn2 or bovine serum albumin (BSA). Under these conditions, up to 1 μM of lcn2 had no effect on the growth of *E. coli* CFT073. Addition of 1 μM lcn2 to the medium rescued the growth of *E. coli* CFT073 treated with 100 nM of Ent-Amp (Figure 8) whereas addition of 1 μM BSA had no effect on Ent-Amp cell killing. These results suggest that lcn2 binds Ent-Amp and blocks its recognition and uptake. To ascertain whether lcn2 binds Ent-Amp in the presence of exogenous Ent, we performed a series of experiments where *E. coli* CFT073 were treated with fixed concentrations of Ent-Amp (100 nM) and lcn2 (1 μM) and the concentration of Ent was varied (0, 0.5, and 1 μM). Ent supplementation restored the antibacterial activity of Ent-Amp (Figure 8). Moreover, When Ent-Amp was combined with a 1:1 molar ratio of Ent and lcn2 at 10-fold excess over the conjugate, no *E. coli* growth was observed, which suggests that lcn2 preferentially binds Ent. Prior work demonstrated that lcn2 cannot bind glucosylated Ent, which was attributed to a steric clash between the glucose moieties and the Ent binding site of the protein,[85] and decreased hydrophobicity of the siderophore may also be a factor. Thus, our data suggest that the nature of linker attachment at C5 and the PEG_3 moiety of Ent-Amp/Amx do no abrogate lcn2 binding as effectively as the glucose moieties exhibited by the salmochelins.

■ SUMMARY AND PERSPECTIVES

Ent-Amp/Amx are two siderophore−β-lactam conjugates based on the native enterobactin scaffold. These molecules hijack siderophore-based iron uptake pathways and provide potent antibacterial activity against various *E. coli* strains, including human pathogens. Our investigations of Ent-Amp/Amx establish the following: (i) Ent-Amp/Amx provide up to 1000-fold enhanced antibacterial activity against *E. coli* strains; (ii) Ent-Amp/Amx are transported into *E. coli* by FepA and potentially other catecholate siderophore receptors (IroN, Iha) employed by pathogenic CTF073 and UTI98; (iii) Ent-Amp/Amx are captured by PBPs in the periplasm, which results in PBP inhibition and cell death; (iv) selective killing of *E. coli* in the presence of less susceptible organisms such as *S. aureus* is achieved because of the enterobactin scaffold; (v) Ent-Amp/Amx exhibit negligible cytotoxicity to human T84 intestinal epithelial cells; and (vi) although lcn2 has the ability to bind Ent-Amp/Amx, this siderophore-scavenging protein prefers to capture native Ent. In total, these studies demonstrate that modification of antibiotic cargo with the native enterobactin platform provides many desirable features for antibiotic delivery and efficacy. The large molecular weight of the conjugates resulting from the native Ent scaffold (as opposed to a smaller mimic) enhances rather than diminishes uptake for Gram-negative *E. coli*. Moreover, we observed no evidence for the development of resistance to Ent-Amp/Amx over the course of the antibacterial activity assays performed during these investigations.

Our studies confirm that the enhanced antibacterial activity observed for Ent-Amp/Amx requires both enterobactin recognition by outer membrane receptors and an intact β-lactam moiety. These results are in accord with expectations. The results are reminiscent of the dramatic antibacterial activity enhancements observed for albomycin, a secondary metabolite produced by *Actinomyces subtropicus*. Albomycin is comprised of the siderophore ferrichrome and a tRNA synthetase inhibitor, and it exhibits antimicrobial activities that are 30,000-fold greater than those of the unmodified tRNA synthetase inhibitor against *E. coli* and *S. aureus*.[99] Nonetheless, the Ent-Amp/Amx cell-killing mechanism may be more complex than only more efficient β-lactam delivery across the Gram-negative outer membrane. Binding of Ent-Amp/Amx to the PBPs presumably results in accumulation of ferric enterobactin in the *E. coli* periplasm for some period of time, which may have deleterious consequences. A recent study of an *E. coli tolC*- mutant revealed that enterobactin accumulation in the periplasm affords growth defects and abnormal cellular morphologies.[100]

A fascinating observation that stems from our current work is the variable susceptibilities and responses of different *E. coli* strains to Ent-Amp/Amx, which contrast the effects of unmodified Amp/Amx. Such differences are manifest in the MIC values to some degree and time-kill kinetics; however, the results presented in Figure 2 indicate that MIC values alone do not provide a full description of how Ent-Amp/Amx susceptibility differs between *E. coli* strains. These results suggest underlying complexity in microbial physiology related to iron-uptake pathways that cannot be fully explained by the

dx.doi.org/10.1021/ja503911p | J. Am. Chem. Soc. 2014, 136, 9677−9691

presence or absence of a gene for a particular receptor (i.e., FepA, IroN). The heightened sensitivity of uropathogenic *E. coli* CFT073 is particularly noteworthy, and it will be interesting to decipher the physiological origins of this effect as well as the differential behavior of various *E. coli* pathogens toward Ent-antibiotic conjugates.

There is a clear and unmet need for new antibacterial agents to treat bacterial infections in humans, including antibiotics that target specific bacterial sub-populations.[1−5] Preventing undesirable consequences of antibiotic treatment on the commensal microbiota, which contributes to human health in beneficial ways, is a challenge that needs to be addressed.[97,98] Such targeted therapeutics will be valuable not only for treating bacterial infections when the causative agent is known (e.g., urinary tract infection and *E. coli*, cystic fibrosis lung infection and *P. aeruginosa*) but also for other pathologies that involve microbial dysbiosis, such as irritable bowel disease.[101] Our studies of Ent-Amp/Amx provide one step toward addressing species-specific antibiotic targeting as well as overcoming Gram-negative outer membrane permeability. From the standpoint of the host environment, commensal *E. coli* employ Ent for acquiring iron in the host, and thus further elaboration of this strategy to specifically target pathogenicity and evade host responses (e.g., lcn2) is desirable. Efforts along these lines are in progress.

■ ASSOCIATED CONTENT

Supporting Information

Experimental details including general synthetic methods, general microbiology materials and methods, and cytotoxicity assays; Tables S1−S3; Figures S1−S25; and NMR spectra. Table S3 summarizes characterization of the Ent-azide and Ent-Amp/Amx molecules, and Figures S18−S25 exhibit analytical HPLC traces for the purified compounds. This material is available free of charge via the Internet at http://pubs.acs.org.

■ AUTHOR INFORMATION

Corresponding Author

lnolan@mit.edu

Notes

The authors declare the following competing financial interest(s): We have submitted a provisional patent application on the enterobactin−antibiotic conjugates described in this work.

■ ACKNOWLEDGMENTS

The Pacific Southwest Regional Center of Excellence for Biodefense and Emerging Infectious Disease, the Searle Scholars Program (Kinship Foundation), and the Department of Chemistry at MIT are gratefully acknowledged for financial support. We thank Prof. M. Raffatellu, Dr. S. Moser, and Dr. A. Wommack for insightful discussions; Prof. K. Poole for *Pseudomonas aeruginosa* PAO1; Prof. L. Cegelski for *E. coli* UTI89; Prof. C. T. Walsh for *E. coli* H9049; and Prof. S. J. Lippard for use of an IR spectrophotometer. We thank J. Bullock, P. Chairatana, and I. Tapescu for providing synthetic precursors to the modified enterobactin platforms. Single-gene knock-out strains of *E. coli* K-12 were obtained from the Keio Collection.[88] NMR instrumentation maintained by the MIT DCIF is supported by NSF grants CHE-9808061 and DBI-9729592.

■ REFERENCES

(1) Walsh, C. T.; Wencewicz, T. A. *J. Antibiot.* **2013**, *67*, 7−22.
(2) Lewis, K. *Nat. Rev. Drug Discovery* **2013**, *12*, 371−387.
(3) Spellberg, B.; Rex, J. H. *Nat. Rev. Drug Discovery* **2013**, *12*, 963−964.
(4) Fischbach, M. A.; Walsh, C. T. *Science* **2009**, *325*, 1089−1093.
(5) Georgopapadakou, N. H. *Expert Opin. Investig. Drugs* **2014**, *23*, 145−148.
(6) Pagès, J.-M.; James, C. E.; Winterhalter, M. *Nat. Rev. Microbiol.* **2008**, *6*, 893−903.
(7) Delcour, A. H. *Biochim. Biophys. Acta* **2009**, *1794*, 808−816.
(8) Hancock, R. E. W. *Trends Microbiol.* **1997**, *5*, 37−42.
(9) Cassat, J. E.; Skaar, E. P. *Cell Host Microbe* **2013**, *13*, 509−519.
(10) Hider, R. C.; Kong, X. *Nat. Prod. Rep.* **2010**, *27*, 637−657.
(11) Miethke, M.; Marahiel, M. A. *Microbiol. Mol. Biol. Rev.* **2007**, *71*, 413−451.
(12) Krewulak, K. D.; Vogel, H. J. *Biochim. Biophys. Acta. Biomembr.* **2008**, *1778*, 1781−1804.
(13) Crouch, M.-L. V.; Castor, M.; Karlinsey, J. E.; Kalhorn, T.; Fang, F. C. *Mol. Microbiol.* **2008**, *67*, 971−983.
(14) Caza, M.; Lépine, F.; Dozois, C. M. *Mol. Microbiol.* **2011**, *80*, 266−282.
(15) Pi, H.; Jones, S. A.; Mercer, L. E.; Meador, J. P.; Caughron, J. E.; Jordan, L.; Newton, S. M.; Conway, T.; Klebba, P. E. *PLoS One* **2012**, *7*, e50020.
(16) Nagy, T. A.; Moreland, S. M.; Andrews-Polymenis, H.; Detweiler, C. S. *Infect. Immun.* **2013**, *81*, 4063−4070.
(17) Dale, S. E.; Doherty-Kirby, A.; Lajoie, G.; Heinrichs, D. E. *Infect. Immun.* **2004**, *72*, 29−37.
(18) Cendrowski, S.; MacArthur, W.; Hanna, P. *Mol. Microbiol.* **2004**, *51*, 407−417.
(19) Raffatellu, M.; George, M. D.; Akiyama, Y.; Hornsby, M. J.; Nuccio, S.-P.; Paixao, T. A.; Butler, B. P.; Chu, H.; Santos, R. L.; Berger, T.; Mak, T. W.; Tsolis, R. M.; Bevins, C. L.; Solnick, J. V.; Dandekar, S.; Baümler, A. J. *Cell Host Microbe* **2009**, *5*, 476−486.
(20) Roosenberg, J. M., II; Lin, Y.-M.; Lu, Y.; Miller, M. J. *Curr. Med. Chem.* **2000**, *7*, 159−197.
(21) Miller, M. J.; Zhu, H.; Xu, Y.; Wu, C.; Walz, A. J.; Vergne, A.; Roosenberg, J. M.; Moraski, G.; Minnick, A. A.; McKee-Dolence, J.; Hu, J.; Fennell, K.; Dolence, E. K.; Dong, L.; Franzblau, S.; Malouin, F.; Möllmann, U. *BioMetals* **2009**, *22*, 61−75.
(22) Ballouche, M.; Cornelis, P.; Baysse, C. *Recent Pat. Anti-infect. Drug Discovery* **2009**, *4*, 190−205.
(23) Ji, C.; Juárez-Hernández, R. E.; Miller, M. J. *Future Med. Chem.* **2012**, *4*, 297−313.
(24) Page, M. G. P. *Ann. N.Y. Acad. Sci.* **2013**, *1277*, 115−126.
(25) Mislin, G. L. A.; Schalk, I. J. *Metallomics* **2014**, *6*, 408−420.
(26) Clevenger, K. D.; Wu, R.; Er, J. A. V.; Liu, D.; Fast, W. *ACS Chem. Biol.* **2013**, *8*, 2192−2000.
(27) Neres, J.; Engelhart, C. A.; Drake, E. J.; Wilson, D. J.; Fu, P.; Boshoff, H. I.; Barry, C. E., III; Gulick, A. M.; Aldrich, C. C. *J. Med. Chem.* **2013**, *56*, 2385−2405.
(28) Alteri, C. J.; Hagan, E. C.; Sivick, K. E.; Smith, S. N.; Mobley, H. L. T. *PLoS Pathog.* **2009**, *5*, e1000586.
(29) Katsu, K.; Kitoh, K.; Inoue, M.; Mitsuhashi, S. *Antimicrob. Agents Chemother.* **1982**, *22*, 181−185.
(30) Neu, H. C.; Labthavikul, P. *Antimicrob. Agents Chemother.* **1983**, *24*, 313−320.
(31) Ohi, N.; Aoki, B.; Shinozaki, T.; Moro, K.; Noto, T.; Nehashi, T.; Okazaki, H.; Matsunaga, I. *J. Antibiot.* **1986**, 230−241.
(32) Ohi, N.; Aoki, B.; Moro, K.; Kuroki, T.; Sugimura, N.; Noto, T.; Nehashi, T.; Matsumoto, M.; Okazaki, H.; Matsunaga, I. *J. Antibiot.* **1986**, 242−250.
(33) Pugsley, A. P.; Zimmerman, W.; Wehrli, W. *J. Gen. Microbiol.* **1987**, *133*, 3505−3511.
(34) Watanabe, N.-A.; Nagasu, T.; Katsu, K.; Kitoh, K. *Antimicrob. Agents Chemother.* **1987**, *31*, 497−504.
(35) Nakagawa, S.; Sanada, M.; Matsuda, K.; Hazumi, N.; Tanaka, N. *Antimicrob. Agents Chemother.* **1987**, *31*, 1100−1105.

(36) Mochizuki, H.; Yamada, H.; Oikawa, Y.; Murakami, K.; Ishiguro, J.; Kosuzume, H.; Aizawa, N.; Mochida, E. *Antimicrob. Agents Chemother.* **1988**, *32*, 1648−1654.
(37) Curtis, N. A. C.; Eisenstadt, R. L.; East, S. J.; Cornford, R. J.; Walker, L. A.; White, A. J. *Antimicrob. Agents Chemother.* **1988**, *32*, 1879−1886.
(38) Nikaido, H.; Rosenberg, E. Y. *J. Bacteriol.* **1990**, *172*, 1361−1367.
(39) Hashizume, T.; Sanada, M.; Nakagawa, S.; Tanaka, N. *J. Antibiot.* **1990**, *43*, 1617−1620.
(40) Silley, P.; Griffiths, J. W.; Monsey, D.; Harris, A. M. *Antimicrob. Agents Chemother.* **1990**, *34*, 1806−1808.
(41) McKee, J. A.; Sharma, S. K.; Miller, M. J. *Bioconjugate Chem.* **1991**, *2*, 281−291.
(42) Diarra, M. S.; Lavoie, M. C.; Jacques, M.; Darwish, I.; Dolence, E. K.; Dolence, J. A.; Ghosh, A.; Ghosh, M.; Miller, M. J.; Malouin, F. *Antimicrob. Agents Chemother.* **1996**, *40*, 2610−2617.
(43) Ghosh, A.; Ghosh, M.; Niu, C.; Malouin, F.; Moellmann, U.; Miller, M. J. *Chem. Biol.* **1996**, *3*, 1011−1019.
(44) Möllmann, U.; Ghosh, A.; Dolence, E. K.; Dolence, J. A.; Ghosh, M.; Miller, M. J.; Reissbrodt, R. *Biometals* **1998**, *11*, 1−12.
(45) Hennard, C.; Truong, Q. C.; Desnottes, J.-F.; Paris, J.-M.; Moreau, N. J.; Abdallah, M. A. *J. Med. Chem.* **2001**, *44*, 2139−2151.
(46) Rivault, F.; Liébert, C.; Burger, A.; Hoegy, F.; Abdallah, M. A.; Schalk, I. J.; Mislin, G. L. A. *Bioorg. Med. Chem. Lett.* **2007**, *17*, 640−644.
(47) Noël, S.; Gasser, V.; Pesset, B.; Hoegy, F.; Rognan, D.; Schalk, I. J.; Mislin, G. L. A. *Org. Biomol. Chem.* **2011**, *9*, 8288−8300.
(48) Ji, C.; Miller, M. J. *Bioorg. Med. Chem.* **2012**, *20*, 3828−3836.
(49) Wittmann, S.; Schnabelrauch, M.; Scherlitz-Hofmann, I.; Möllman, U.; Ankel-Fuchs, D.; Heinisch, L. *Bioorg. Med. Chem.* **2002**, *10*, 1659−1670.
(50) Möllman, U.; Heinisch, L.; Bauernfeind, A.; Köhler, T.; Ankel-Fuchs, D. *Biometals* **2009**, *22*, 615−624.
(51) Yoganathan, S.; Sit, C. S.; Vederas, J. C. *Org. Biomol. Chem.* **2011**, *9*, 2133−2141.
(52) Alt, S.; Burkard, N.; Kulik, A.; Grond, S.; Heide, L. *Chem. Biol.* **2011**, *18*, 304−313.
(53) Ji, C.; Miller, P. A.; Miller, M. J. *J. Am. Chem. Soc.* **2012**, *134*, 9898−9901.
(54) Zeng, Y.; Kulkarni, A.; Yang, Z.; Patil, P. B.; Zhou, W.; Chi, X.; Van Lanen, S.; Chen, S. *ACS Chem. Biol.* **2012**, *7*, 1565−1575.
(55) Wencewicz, T. A.; Long, T. E.; Möllmann, U.; Miller, M. J. *Bioconjugate Chem.* **2013**, *24*, 473−486.
(56) Wencewicz, T. A.; Miller, M. J. *J. Med. Chem.* **2013**, *56*, 4044−4052.
(57) Juárez-Hernández, R. E.; Miller, P. A.; Miller, M. J. *ACS Med. Chem. Lett.* **2012**, *3*, 799−803.
(58) Milner, S. J.; Seve, A.; Snelling, A. M.; Thomas, G. H.; Kerr, K. G.; Routledge, A.; Duhme-Klair, A.-K. *Org. Biomol. Chem.* **2013**, *11*, 3461−3468.
(59) Yu, Y.; Wong, J.; Lovejoy, D. B.; Kalinowski, D. S.; Richardson, D. R. *Clin. Cancer Res.* **2006**, *12*, 6876−6883.
(60) Manning, T.; Kean, G.; Thomas, J.; Thomas, K.; Corbitt, M.; Gosnell, D.; Ware, R.; Fulp, S.; Jarrard, J.; Phillips, D. *Curr. Med. Chem.* **2009**, *16*, 2416−2429.
(61) Braun, V.; Pramanik, A.; Gwinner, T.; Köberle, M.; Bohn, E. *BioMetals* **2009**, *22*, 3−13.
(62) Thomas, X.; Destoumieux-Garzón, D.; Peduzzi, J.; Afonso, C.; Blond, A.; Birlirakis, N.; Goulard, C.; Dubost, L.; Thai, R.; Tabet, J.-C.; Rebuffat, S. *J. Biol. Chem.* **2004**, *279*, 28233−28242.
(63) Tomaras, A. P.; Crandon, J. L.; McPherson, C. J.; Banevicius, M. A.; Finegan, S. M.; Irvine, R. L.; Brown, M. F.; O'Donnell, J. P.; Nicolau, D. P. *Antimicrob. Agents Chemother.* **2013**, *57*, 4197−4207.
(64) Miller, M. J.; Walz, A. J.; Zhu, H.; Wu, C.; Moraski, G.; Möllmann, U.; Tristani, E. M.; Crumbliss, A. L.; Ferdig, M. T.; Checkley, L.; Edwards, R. L.; Boshoff, H. I. *J. Am. Chem. Soc.* **2011**, *133*, 2076−2079.
(65) Raymond, K. N.; Dertz, E. A.; Kim, S. S. *Proc. Natl. Acad. Sci. U.S.A.* **2003**, *100*, 3584−3588.
(66) Zheng, T.; Bullock, J. L.; Nolan, E. M. *J. Am. Chem. Soc.* **2012**, *134*, 18388−18400.
(67) Ramirez, R. J. A.; Karamanukyan, L.; Ortiz, S.; Gutierrez, C. G. *Tetrahedron Lett.* **1997**, *38*, 749−752.
(68) Butler, D. L.; Jakielaszek, C. J.; Miller, L. A.; Poupard, J. A. *Antimicrob. Agents Chemother.* **1999**, *43*, 283−286.
(69) Goetz, D. H.; Holmes, M. A.; Borregaard, N.; Bluhm, M. E.; Raymond, K. N.; Strong, R. K. *Mol. Cell* **2002**, *10*, 1033−1043.
(70) Brochu, A.; Brochu, N.; Nicas, T. I.; Parr, T. R., Jr.; Minnick, A. A., Jr.; Dolence, E. K.; McKee, J. A.; Miller, M. J.; Lavoie, M. C.; Malouin, F. *Antimicrob. Agents Chemother.* **1992**, *36*, 2166−2175.
(71) Shanzer, A.; Libman, J. *J. Chem. Soc., Chem. Commun.* **1983**, 846−847.
(72) Fernández-González, A.; Badía, R.; Díaz-García, M. E. *Anal. Biochem.* **2005**, *341*, 113−121.
(73) Chan, T. R.; Hilgraf, R.; Sharpless, K. B.; Fokin, V. V. *Org. Lett.* **2004**, *6*, 2853−2855.
(74) Staub, I.; Sieber, S. A. *J. Am. Chem. Soc.* **2008**, *130*, 13400−13409.
(75) Pearson, H. A.; Urban, M. W. *J. Mater. Chem. B* **2014**, *2*, 2084−2087.
(76) Kaper, J. B.; Nataro, J. P.; Mobley, H. L. T. *Nat. Rev. Microbiol.* **2004**, *2*, 123−140.
(77) Flo, T. H.; Smith, K. D.; Sato, S.; Rodriguez, D. J.; Holmes, M. A.; Strong, R. K.; Akira, S.; Aderem, A. *Nature* **2004**, *432*, 917−921.
(78) Mulvey, M. A.; Schilling, J. D.; Hultgren, S. J. *Infect. Immun.* **2001**, *69*, 4572−4579.
(79) Mobley, H. L. T.; Green, D. M.; Trifillis, A. L.; Johnson, D. E.; Chippendale, G. R.; Lockatell, C. V.; Jones, B. D.; Warren, J. W. *Infect. Immun.* **1990**, *58*, 1281−1289.
(80) Henderson, J. P.; Crowley, J. R.; Pinkner, J. S.; Walker, J. N.; Tsukayama, P.; Stamm, W. E.; Hooton, T. M.; Hultgren, S. J. *PLoS Pathog.* **2009**, *5*, e1000305.
(81) Müller, S. I.; Valdebenito, M.; Hantke, K. *Biometals* **2009**, *22*, 691−695.
(82) Baümler, A. J.; Tsolis, R. M.; van der Velden, A. W. M.; Stojiljkovic, I.; Anic, S.; Heffron, F. *Gene* **1996**, *183*, 207−213.
(83) Hantke, K.; Nicholson, G.; Rabsch, W.; Winkelmann, G. *Proc. Natl. Acad. Sci. U.S.A.* **2003**, *100*, 3677−3682.
(84) Rabsch, W.; Voigt, W.; Reissbrodt, R.; Tsolis, R. M.; Baümler, A. J. *J. Bacteriol.* **1999**, *181*, 3610−3612.
(85) Fischbach, M. A.; Lin, H.; Zhou, L.; Yu, Y.; Abergel, R. J.; Liu, D. R.; Raymond, K. N.; Wanner, B. L.; Strong, R. K.; Walsh, C. T.; Aderem, A.; Smith, K. D. *Proc. Natl. Acad. Sci. U.S.A.* **2006**, *103*, 16502−16507.
(86) Berger, T.; Togawa, A.; Duncan, G. S.; Elia, A. J.; You-Ten, A.; Wakeham, A.; Fong, H. E. H.; Cheung, C. C.; Mak, T. W. *Proc. Natl. Acad. Sci. U.S.A.* **2006**, *103*, 1834−1839.
(87) Garcia, E. C.; Brumbaugh, A. R.; Mobley, H. L. T. *Infect. Immun.* **2011**, *79*, 1225−1235.
(88) Baba, T.; Ara, T.; Hasegawa, M.; Takai, Y.; Okumura, Y.; Baba, M.; Datsenko, K. A.; Tomita, M.; Wanner, B. L.; Mori, H. *Mol. Syst. Biol.* **2006**, 2006.0008.
(89) Thulasiraman, P.; Newton, S. M. C.; Xu, J.; Raymond, K. N.; Mai, C.; Hall, A.; Montague, M. A.; Klebba, P. E. *J. Bacteriol.* **1998**, *180*, 6689−6696.
(90) Abergel, R. J.; Zawadzka, A. M.; Hoette, T. M.; Raymond, K. N. *J. Am. Chem. Soc.* **2009**, *131*, 12682−12692.
(91) Robinson-Fuentes, V. A.; Jefferies, T. M.; Branch, S. K. *J. Pharm. Pharmacol.* **1997**, *49*, 843−851.
(92) Poole, K.; Young, L.; Neshat, S. *J. Bacteriol.* **1990**, *172*, 6991−6996.
(93) Dean, C. R.; Neshat, S.; Poole, K. *J. Bacteriol.* **1996**, *178*, 5361−5369.
(94) Ghysels, B.; Ochsner, U.; Möllman, U.; Heinisch, L.; Vasil, M.; Cornelis, P.; Matthijs, S. *FEMS Microbiol. Lett.* **2005**, *246*, 167−174.

(95) Sebulsky, M. T.; Heinrichs, D. E. *J. Bacteriol.* **2001**, *183*, 4994−5000.
(96) Zawadzka, A. M.; Abergel, R. J.; Nichiporuk, R.; Andersen, U. N.; Raymond, K. N. *Biochemistry* **2009**, *48*, 3645−3657.
(97) Sekirov, I.; Russell, S. L.; Antunes, L. C. M.; Finlay, B. B. *Physiol. Rev.* **2010**, *90*, 859−904.
(98) Rafii, F.; Sutherland, J. B.; Cerniglia, C. E. *Ther. Clin. Risk Manag.* **2008**, *4*, 1343−1357.
(99) Stefanska, A. L.; Fulston, M.; Houge-Frydrych, C. S. V.; Jones, J. J.; Warr, S. R. *J. Antibiot.* **2000**, *53*, 1346−1353.
(100) Vega, D. E.; Young, K. D. *Mol. Microbiol.* **2014**, *91*, 508−521.
(101) Chassaing, B.; Koren, O.; Carvalho, F. A.; Ley, R. E.; Gewirtz, A. T. *Gut* **2014**, *63*, 1069−1080.